METMINEC (PTY) LTD
MINING THE FUTURE

TANZANIA LITHIUM EXPLORATION

HOMBOLO PROJECT

Geology Report

Authors:

Nndanduleni Muavhi: MSc (Geology)
Clifford Mosala: B.Tech. (Geology)
Permly Shingange: B.Tech. (Geology), MTech (Geophysics)
Mixo Vukeya BSc Hons (Geology)

Reviewed by:

Dr Gerhard Du Plessis: BSc Hons, MSc, PhD

Approved by:

Godfrey Mothapo: BSc Hons (Geology), MSc (Eng.), BA (Econ)

Name and Signature of the Project Leader:

……

Makgamatho Godfrey Mothapo Pr. Sci. Nat

Date: 14 February 2024

Table of Contents

EXECUTIVE SUMMARY 4

1. INTRODUCTION 6
   1.1. Description of the project area 6
2. GEOLOGICAL SETTING 7
   2.1. Regional geology 7
   2.2. Local geology 9
3. OCCURRENCE OF LITHIUM ORE IN NATURE 9
   3.1. Pegmatite deposits 10
   3.2. Formation of pegmatite deposits 10
   3.3. Pegmatite deposit types 11
4. A REVIEW OF EXPLORATION TOOLS FOR PEGMATITE DEPOSIT 13
   4.1. Remote sensing 13
   4.2. Field mapping and sampling 14
   4.3. Using whole rock geochemistry as an exploration tool for pegmatite deposits 15
   4.4. Using mineralogy as an exploration tool for pegmatite deposits 17
5. METHODOLOGY 17
   5.1. Reconnaissance survey 18
   5.2. Field mapping and sampling 19
   5.3. Sample analysis 22
6. RESULTS 23
   6.1. Field mapping results 23
   6.2. Geochemical results 27
      6.2.1. Assessment of potential lithium enrichment in the project area 27
      6.2.2. Assessment of potential enrichment of other economic metals in the project area .. 37
7. CONCLUSIONS 40
8. RECOMMENDATIONS 41
9. REFERENCES 43

List Of Figures

Figure 1: Locality map of the project area. 6
Figure 2: Tectonic region underlying the project area (KMB: Kariba Mobile Belt; MMB: Mozambique Mobile Belt). 8
Figure 3: Geology of the project area. Superimposed pegmatite deposits and Hombolo Lithium Block from Auroch Minerals LTD (2016). 9
Figure 4: Potential lithium-bearing areas in the project area generated from the processing of LANDSAT images. 18
Figure 5: Prioritized block in red. 19
Figure 6: Predetermined traverse lines for field mapping. 20
Figure 7: Some of the sampled outcrops (the lithologies entitled pegmatites are suspected pegmatites). 21
Figure 8: Sampled points to date. 22
Figure 9: Geological map. 24
Figure 10: Granite outcrop. 25
Figure 11: Porphyritic leucogranite outcrop. 25
Figure 12: Pegmatitic granite. 26
Figure 13: Pegmatite in contact with a silicified granite. 27
Figure 14: A bar graph showing the Li contents of the samples from the project area. 28
Figure 15: Radar graphs showing Mg/Li and K/Ba ratio values for samples with Li content of >20. 30
Figure 16: Radar graphs showing Mg/Li and K/Ba ratio values for samples with Li content of <20. 32
Figure 17: K vs Ca and Mg vs Ca binary plots of samples with Li content of > 20 ppm. The black line represents the biotite gness trend from Chukwe and Obiara (2021). 35
Figure 18: K vs Ca and Mg vs Ca binary plots of samples with Li content of < 20 ppm. 36

List Of Tables

Table 1: Average trace element contents of upper continental crust (Taylor and McLennan, 1985). 15
Table 2: Range of trace element contents and rare element ratios in fertile granites and rare element pegmatites (Černý, 1989). 16
Table 3: Selected elemental contents and ratio values of samples of the current work. 29
Table 4: Selected major and trace elements and ratios of different rock types from Chukwu and Obiora (2021) and Chen et al. (2024). 34
Table 5: Samples with traces of Be. 38

EXECUTIVE SUMMARY

METMINEC (Pty) Ltd was appointed by **CGRA Mining Inc.** to execute an exploration project to determine potential Lithium (Li) deposits in the prospecting concession of ID: PL_17271_2021 in the Dodoma Region, Tanzania. Prospecting in this concession area was prioritized due to the high potential of hosting lithium deposits following the processing and interpretation of LANDSAT 8 (OLI) images (Muavhi et al., 2023). The processing of Landsat images was achieved using ENVI software.

Field mapping and sampling have been completed. The concession is characterized by pegmatites, granites, migmatites, granite porphyries, granitic gneisses, and isolated amphibolite in the shear zones. All lithologies observed in the concession have been sampled and samples were submitted to the laboratory for analysis, due to analytical limitations all samples were subjected to IPC-OES analysis.

The analysis of whole-rock geochemistry of rock samples is considered an excellent tool to distinguish between barren granite and fertile granite and to evaluate the degree of fractionation which is responsible for rare element enrichment in pegmatites. Ratios that are considered excellent fractionation indicators of rare element enrichment are K/Rb, K/Cs, Nb/Ta, K/Ba and Mg/Li.

Out of twenty-four analyzed samples, twenty-two samples show traces of Li content with HMB 012 attaining the highest Li content (44 ppm). Most samples have Mg/Li and K/Ba ratios within the range that indicate potential rare element enrichment. These include HMB 014, HMB 016, HMB 017, HMB 018, HMB 022, HMB 024 and HMB 025. Also, some of these samples correspond to Mg, K, and Ca contents of known rare element pegmatites (from previous studies) in Ca vs K and Mg vs Ca binary plots.

In addition, HMB 024 and HMB 007 showed high contents of Sn. Tin value as high as 35 ppm is considered a good indicator of a potential Sn ore. Therefore, the Sn contents of HMB 024 and HMB 007 present a potential to recognize existing Sn-bearing zones in their outcrops.

Although the results do not permit a comprehensive understanding of the geological context of the collected samples, they do, however, provide preliminary insights into the existing potential of rare element enrichment associated with the increase in the degree of fractionation in the area. As a result, it is recommended to conduct follow-up exploration, especially in areas with the potential for rare element enrichment.

Metminec recommends that the samples be sent to South Africa to be analyzed at the SGS Laboratory utilizing the ICP-MS instrument. ICP-MS provides high precision and accuracy of element analysis. We also recommend the use of the XRD (X-ray diffraction) analytical technique XRD is useful in identifying and quantifying minerals rock samples. It is further recommended to conduct follow-up sampling and trenching (or drilling) at points displaying traces of Li and critical metals.

1. INTRODUCTION

METMINEC (Pty) Ltd was appointed by **CGRA Mining Inc.** to execute an exploration project to determine potential Lithium (Li) deposits in the prospecting concession of ID: PL_17271_2021 in the Dodoma Region, Tanzania. Prospecting in this concession area was prioritized due to the high potential of hosting lithium deposits following the processing and interpretation of LANDSAT 8 (OLI) images (Muavhi et al., 2023).

1.1. Description of the project area

The project area (prospecting concession of ID: PL_17271_2021) is located next to Hombolo which is situated about 30 km northeast of the capital city, Dodoma (Figure 1).

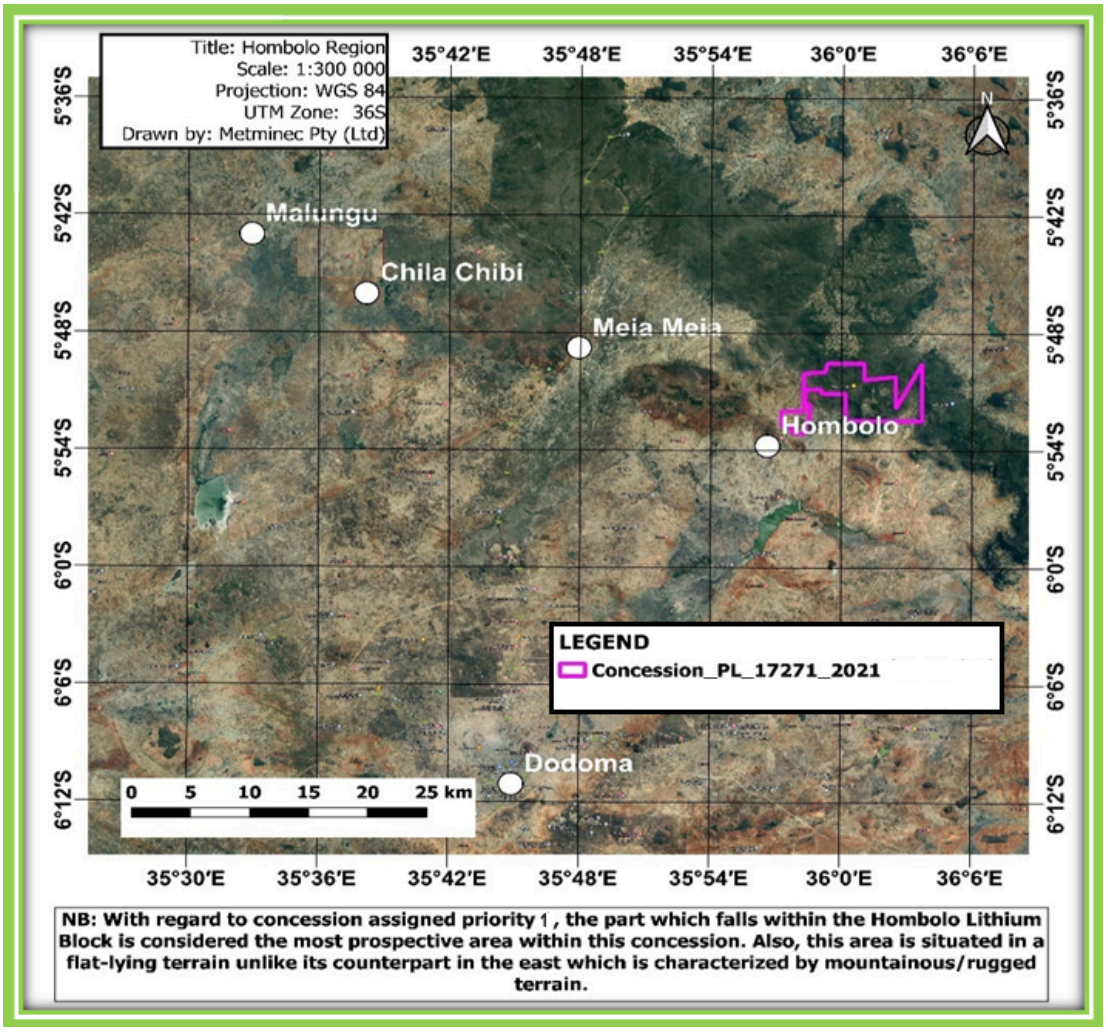

Figure 1: Locality map of the project area.

The project area is generally mountainous with flat-lying blocks in the southwestern part of the area. The elevation ranges from 1125 to 1850 m above sea level. The area is characterized by thick vegetation, especially in the mountainous region.

Access to the project area is via the gravel secondary road which passes through the area and joins the A104 Main Road to the west. The project area extends over an area of 2600 hectares (See Figure 1).

The area receives the highest rainfall in December and has an average rainfall of 587 mm throughout the year, recharging the ephemeral streams in the project area. The area receives little to no rain from June to September, with May and June being the coldest months with an average high temperature of 27.2°C.

The warmest month (with the highest average high temperature) is October (31.8°C) (Weather Atlas).

2. GEOLOGICAL SETTING

2.1. Regional geology

Regionally, the project area is situated within the East African Rift (EAR) (Figure 2).

Tanzania Craton is located in the center of EAR. This craton is bound to the east and west by the Mozambique Mobile Belt and Kariba Mobile Belt, respectively.

Tanzania Craton comprises Palaeo-to Mesoarchean basement which is largely characterized by diorite to granodiorite ortho gneisses with inclusions of supracrustal rocks. This basement is overlain by granitoid-greenstone belts (~2700 Ma) in northern and central Tanzania (von Knorring and Condliffe, 1987).

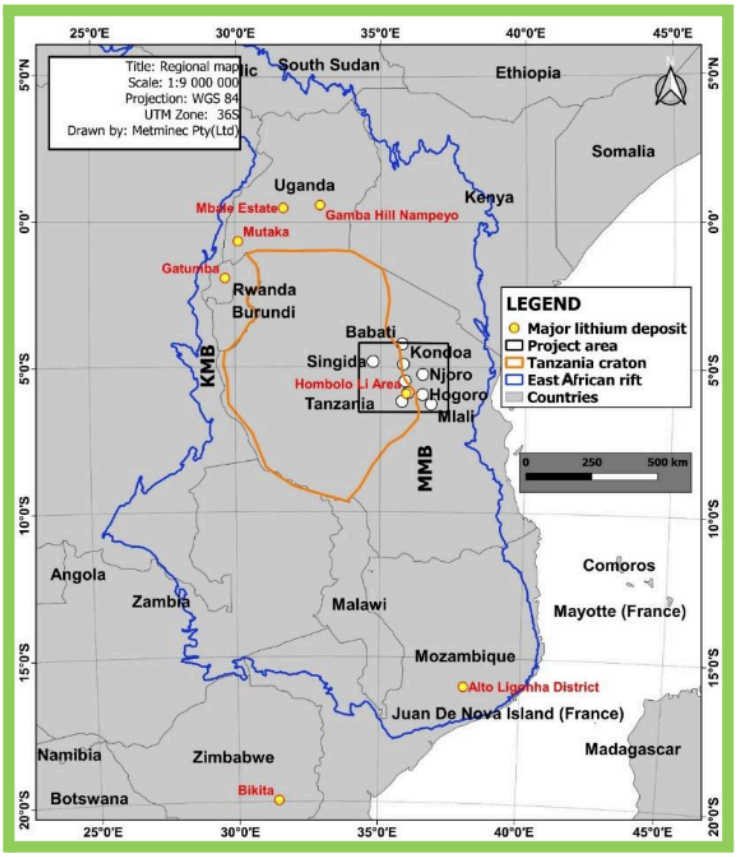

Figure 2: Tectonic region underlying the project area (KMB: Kariba Mobile Belt; MMB: Mozambique Mobile Belt).

Mineralized pegmatites occur in cratons which have remained stable over the past 1500 Ma – as well as in the comparatively younger orogens, consisting of mobile zones that have undergone several orogenic deformations during the past 1200 Ma. For example, the lithium-bearing pegmatites of Bikita in Zimbabwe are found in the much older basement rocks of the Zimbabwe Craton (von Knorring and Condliffe, 1987). Hombolo is one of the cratonic hosts of lithium-bearing pegmatites. However, the most extensive mineralized pegmatite areas so far known are associated with the younger orogens such as the Kariba Mobile Belt and Mozambique Mobile Belt (Figure 2) (von Knorring and Condliffe, 1987).

In the Mozambique Mobile Belt, the major lithium pegmatite area is the Alto Ligonha region in Mozambique which has mineralized lithium pegmatites of Muiane, Mutala, Morrua, and Marropino. On the other hand, Kariba Mobile Belt is host to Gatumba pegmatites in Rwanda and Mutaka, Mable Estate, and Gamba Hill Nampeyo in Uganda (Figure 2) (von Knorring and Condliffe, 1987). Tectonically and historically, the project area is situated in a region with favorable geological conditions for lithium deposit occurrences.

2.2. Local geology

The project area forms part of Tanzania craton which is a host to several known lithium-bearing pegmatites around Hombolo. The area is along the Hombolo-Msangani belt which is also linked to lithium-bearing pegmatites. In terms of surface geology, the area is characterized predominately by granites, migmatites, and undifferentiated soils including mafic dykes (Figure 3). Granites and migmatites host gneiss and amphibolite which is reportedly known to host lithium-bearing pegmatites around the Hombolo Lithium Block (von Knorring and Condliffe, 1987; Auroch Minerals LTD, 2016).

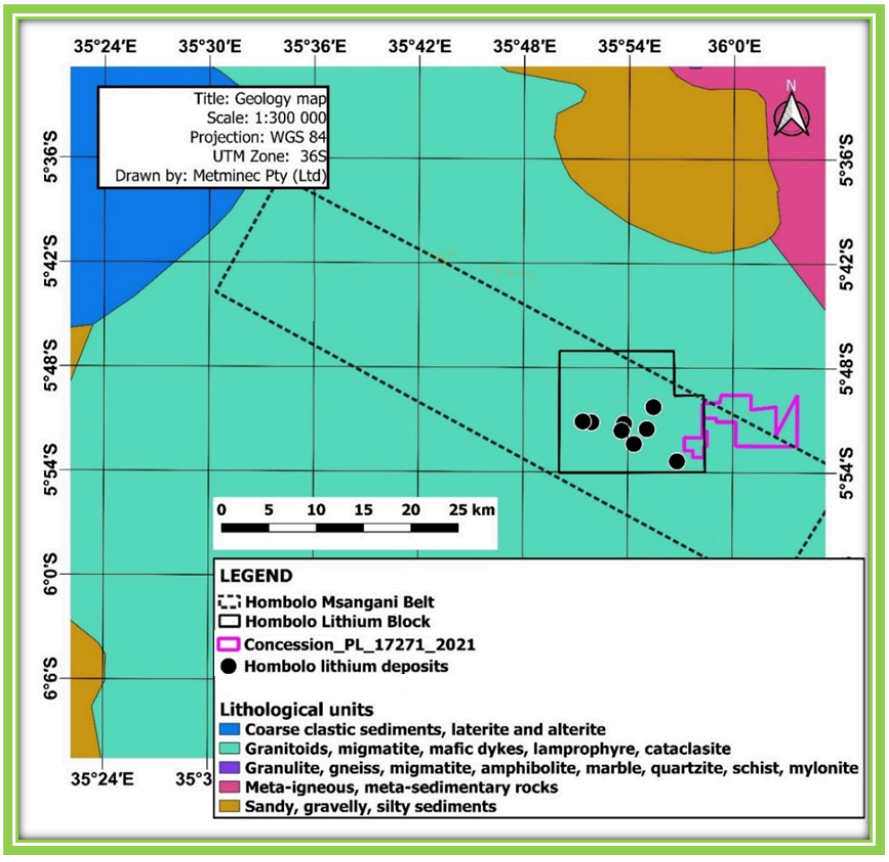

Figure 3: Geology of the project area. Superimposed are pegmatite deposits and Hombolo Lithium Block).

3. OCCURRENCE OF LITHIUM ORE IN NATURE

Lithium ore is a type of rock or mineral that contains significant concentrations of lithium, a soft, silver-white alkali metal (Mat, 2023). This metal is known for its unique properties such as low density, strong corrosion resistance, and fatigue resistance; thus, making lithium a basic raw material for various resources, such as light alloys, atomic reactors, and lithium batteries.

With the increase of strategic emerging industries, such as aerospace, and its use in nuclear and new forms of energy, the demand for lithium has steadily risen, which further highlights its use (Chen et al., 2023). Consequently, this has increased the exploration of lithium resources and research on accessing lithium resources worldwide.

In general, lithium is a relatively rare element, although it is naturally found in various geological settings, but always in very low concentrations (Garrett, 2004). The average amount of lithium in the Earth's upper crust has been estimated to be as low as 20 ppm (Vine, 1980) and as high as 60 ppm (Deberitz, 1993). The economic lithium resources are typically found in pegmatites, sedimentary and brine deposits (Adibhatla et al., 2023).

3.1. Pegmatite deposits

Pegmatites are holocrystalline rocks typically composed of igneous rock-forming minerals that are, in part, very coarse-grained, although some are extremely varied in grain size and show an abundance of crystals with skeletal, graphic, or other strongly directional growth habits. They are commonly granitic in composition, consisting mainly of quartz, feldspar, and mica.

Pegmatites are an important source of rare metals including tin, tantalum, niobium, beryllium, cesium, rubidium, scandium, thorium, uranium, and rare earth in addition to lithium (London, 2008). Most of these metals are considered to be strategic metals which refer to metals that are of greatest risk to supply disruptions or are important to a country's economy or defense (Linnen et al., 2012).

3.2. Formation of pegmatite deposits

The formation of pegmatites is associated with:

1) Fractional crystallization of granitic magma plutons; and

2) Partial melting of crustal or mantle rocks involving the presence of fluids (London, 2005).

In the first setting, the siliceous melt is separated from parental granites by filter pressing and

intrudes into meta-sedimentary country rocks, where the melt crystallizes and forms either zoned or unzoned pegmatites (Dill, 2015). The concentration of fluxing elements, such as P, B, F, Li, and H_2O, reduces the viscosity and solidus temperature of the melt, but increases the solubility of large-ion-lithophile elements (LILE) (e.g., K, Rb, Cs, Ba, etc.) and high-field-strength elements (HSFE) (Zr, Nb, REE, Hf, Ta, etc.). Depending on the temperature, the incompatible elements (LILE and HSFE) precipitate and form minerals when fluxing elements are removed from the melt by chemical quenching (Steiner, 2019).

In the second setting, pegmatites are derived by partial melting rather than fractional crystallization of a parent granite or nearby S-type granite. This type of pegmatite is associated with the transition between pure magmatic fractionation and hydrothermal alteration, which plays a significant role in localizing economically significant mineralization of Sn, W, Li, Cs, Ta, Nb, etc. (Steiner, 2019).

It is important to note, however, that several factors control whether or not a fractional crystallization or partial melting will produce a fertile granite melt and later a pegmatite melt. These factors include (Selway and Breaks, 2005):

- *Composition of melt:* Fertile granites are derived from a peraluminous S-type granitic melt.
- *Degree of partial melting:* Fertile granites require a high degree of partial melting of the source rock that produced the magma.
- *Degree of fractionation:* A high degree of fractionation is required to concentrate incompatible rare elements and volatiles in a granitic melt to crystallize a rare element pegmatite.

3.3. Pegmatite deposit types

Although pegmatites are widespread and relatively common, rare element pegmatites (i.e. pegmatites of economic interest) make up only about 0.1% (Laznicka, 2006).

Rare element pegmatites can be divided into two compositional categories which differ in terms of the geological processes responsible for rare element mineralization (Duuring, 2020):

- *Lithium–cesium–tantalum (LCT):* LCT pegmatites are enriched in Li, Cs, Ta, Be, B, F, P, Mn, Ga, Rb, Nb, Sn and Hf. Examples of major LCT pegmatite deposits in Africa include Bikita in Zimbabwe Craton, Alito Ligonha in Mozambique Mobile Belt (MMB), and Manono-Kitolo (Democratic Republic of Congo) and Gatumba (Burundi) in Kariba Mobile Belt (KMB) (Dwight et al., 2010). LCT pegmatites account for about one-fourth of the world's lithium production (Naumova and Naumova, 2010), one-tenth of the beryllium (Foley et al., 2016), most of the tantalum and all of the cesium (USGS, 2011).

- *Niobium–yttrium–fluorine (NYF):* NYF pegmatites are enriched in Be, Sn, B, Nb > Ta, Ti, Y, rare earth elements, Zr, Th, U, Sc, and F, but are depleted in Li, Cs, P, B, and Rb. Biotite is more common in NYF pegmatites, while muscovite is dominant in LCT pegmatites. Notable NYF pegmatite deposits in the world include the South Platte granite and pegmatite system in the Grötingen granite and Abborselet and other associated pegmatites in Sweden, the Lac du Bonnet biotite granite and Shatford Lake pegmatite group in Canada, and the Stockholm granite and Ytterby pegmatite group, Sweden (Duuring, 2020).

- Mixed or hybrid rare element pegmatites: Mixed pegmatites have blended rare element signatures and are considered to be products of contamination of NYF and LCT pegmatites at the magmatic or post-magmatic stage. For example, they have been suggested to result from the re-melting of newly formed NYF pegmatites by metasomatic fluids rich in Li, B, Ca, and Mg. Some examples of mixed pegmatites include those at Kimito in Finland, the Tørdal district of Norway, and the O'Grady batholith in Canada (Duuring, 2020).

In terms of economic extraction of lithium in pegmatites, grades of about 1% Li_2O have historically been required for economic extraction, although lower grades have been acceptable in pegmatites that produce more than one metal. Spodumene (LiAlPO4 (F, OH)) is the most important lithium mineral in pegmatites including lepidolite (KLi2AlSi4O10F2) and petalite (LiAlSi4O10) (Kesler, 2012).

4. A REVIEW OF EXPLORATION TOOLS FOR PEGMATITE DEPOSIT

Mineral exploration normally begins with information gathering and desktop studies including Geographic Information System (GIS) data reviews.

Following the identification of prospective regional areas, initial targets are verified in the field by geological mapping and geochemical sampling.

Detailed geochemical sampling of rock, soil, and stream sediments and subsequent analyses represent the most important tools for providing insights about the enrichment of elements of economic interest (Steiner, 2019).

Below we discuss some of the tools that can be employed during the exploration of pegmatite deposits.

4.1. Remote sensing

Remote sensing is the science of obtaining, processing, and interpreting images, and related data, acquired from aircraft and satellites that record the interaction between matter and electromagnetic energy. Remote sensing images are used for mineral exploration in three applications (Sabins, 1999):

1) To map geology;

2) To map the faults and fractures that localize ore deposits and

3) To recognize minerals by their spectral signature.

The advantage of remote sensing over traditional exploration methods is that the former is fast and cheap in gathering lithological and mineralogical information over a wide region including areas that are considered inaccessible. As a result, this technique has been widely and successfully applied in locating follow-up targets for potential mineral deposits at an earlier stage of mineral exploration (Ali and Pour, 2014; Fernandes et al., 2017; Muavhi et al., 2021).

The application of remote sensing in the mapping of these mineral targets depends on the

capacity and capability of a sensor to register spectral signatures related to minerals associated with such deposits (Muavhi et al., 2021). This technique is mainly used to map minerals associated with hydrothermal alteration zones of copper and gold deposits, with limited published work on the mapping of potential lithium-bearing areas. Nonetheless, recently few studies have demonstrated the capabilities of this technique in successfully mapping lithium-bearing potential areas (e.g., Ali and Pour, 2014; Fernandes et al., 2019).

Fernandes et al. (2019) proposed several Landsat band ratios for mapping potential lithium-bearing minerals. These authors proposed Landsat band 3/band5 and band 4/band7 to map spodumene and lepidolite, respectively. The work was conducted at the Fregeneda (Salamanca, Spain)-Almendra (Vila Nova de Foz Côa, Portugal) region, where different known types of lithium-bearing pegmatites exist. The authors also discussed the limitations of the methodology proposed, but overall, they demonstrated the ability of remote sensing in the identification of follow-up targets for lithium deposit exploration. The limitation emphasized by Fernandes et al. (2019) is the similar response of lithium-bearing materials and some urbanized areas and agricultural fields observed in resultant images. The approach proposed by Fernandes et al. (2019) was implemented during a desktop study and led to the prioritization of the project area.

4.2. Field mapping and sampling

Every exploration step is of great significance since the exploration program is usually made up of interrelated and interdependent steps.

Geological mapping and sampling are very crucial as they are the main tools to verify the targets initially generated through desktop study/remote sensing/geophysical surveys.

As stated previously, detailed geochemical sampling of rock, soil, and stream sediments and subsequent analyses represent the most important tools for providing insights about the enrichment of elements of economic interest (Steiner, 2019).

4.3. Using whole rock geochemistry as an exploration tool for pegmatite deposits

The analysis of whole rock geochemistry is an excellent tool to distinguish between barren granite and fertile granite and to evaluate the degree of fractionation of a rare element pegmatite (Selway and Breaks, 2005).

The Major and trace element geochemistry of samples can be utilized to assess the degree of fractionation of fertile granites and rare-element pegmatite. The CaO-Na_2O-K_2O ternary diagram is normally used to determine which alkali or alkali earth element (K/Ca/Na) is dominant.

Rare earth element pegmatites have high K contents relative to Ca and Na. On the contrary, barren granites are characterized by low K contents and high contents of Ca and Na.

In general, rare-earth elements that are at least three times that of the average upper continental crust (Table 1) are of interest for pegmatite exploration.

The increase in degree of fractionation is responsible for the enrichment of rare element contents such as Li, Be, B, F, P, Ga, Rb, Cs, Y, Nb, Sn, REE and Ta; and the decrease of elements such as Ti, Sr, Ba, and Zr (Černý and Meintzer, 1988; Selway and Breaks, 2005; Chukwu and Obiora, 2021; Chen et al., 2024).

Trace element	Ppm
Li	20
Cs	3.7
Ta	2.2
Nb	25
Be	3
Rb	112
Sn	5.5
Ga	17
K/Cs	7630
K/Rb	25.2
Nb/Ta	11.4

Table 1: Average trace element contents of upper continental crust (Taylor and McLennan, 1985).

The ranges of trace element contents and trace element ratios of fertile granite and rare element pegmatites are given in Table 2.

Trace element	Ppm	Element ratio	Ppm
Ti	<100 – 4300	**K/Rb**	42 – 270
Sr	<1 – 1445	**K/Cs**	1600 – 15400
Ba	6 – 900	**K/Ba**	48 – 18200
Zr	<1 – 77	**Rb/Sr**	1.6 – 185
Li	1 – 3500	**Mg/Li**	1.7 – 50
Be	1 – 604	**Al/Ga**	1180 - 3100
Ga	19 – 90	**Zr/Hf**	14 – 64
Rb	32 – 5775		
Cs	3 – 51		
Y	3 – 102		
Sn	<1 – 112		

Table 2: Range of trace element contents and rare element ratios in fertile granites and rare element pegmatites (Černý, 1989).

The most important ratios that are considered excellent fractionation indicators are K/Rb, K/Cs, Nb/Ta, and Mg/Li (Table 2), all of which should be significantly lower than average upper continental crust (Table 1) in fertile granitic systems (Selway and Breaks, 2005; Chukwu and Obiora, 2021; Chen et al., 2024). For example, the fertile granite has an average Nb/Ta ratio of 4.3 with a range from 0.8 to 8.4 (Breaks and Tindle, 1997), whereas Nb/Ta for the average upper continental crust is 11.4. Pegmatites with the greatest economic potential for LCT will have very low K/Rb, K/Cs, Nb/Ta, and Mg/Li ratios (Selway and Breaks, 2005; Chukwu and Obiora, 2021; Chen et al., 2024).

The Mg/Li ratio for whole rock geochemistry analysis is one of the best indicators of the degree of fractionation of granites and pegmatites.

According to Černý (1989), Mg/Li ratios less than 30 indicate a high degree of fractionation. An elevated Mg/Li ratio (e.g., Mg/Li = 50) indicates abundant Mg in a primitive rock (barren granite), whereas a low Mg/Li ratio (e.g., Mg/Li < 10) indicates elevated Li contents in an evolved rock (fertile granite) (Selway and Breaks, 2005).

4.4. Using mineralogy as an exploration tool for pegmatite deposits

As a granitic melt crystallizes and fractionates, minerals become enriched in rare elements. K-feldspar and muscovite become enriched in Rb and Cs; garnet becomes enriched in Mn; and apatite becomes enriched in F. Increasing fractionation also results in crystallization of Li-Be-B-Ta-Cs bearing minerals such as Li-rich minerals (i.e., spodumene, petalite, lepidolite, elbaite, liddicoatite, amblygonite/montebrasite, and lithiophilite), beryl (Be), and tourmaline (B), pollucite (Cs) and Ta-rich minerals such as manganotantalite, ferrotapiolite, microlite, and wodginite.

The presence of common rock-forming minerals with elevated contents of rare elements in fertile granites is often the first clue in exploring blind or buried pegmatite deposits (Selway and Breaks, 2005).

5. METHODOLOGY

As stated in the Introduction, the project area was prioritized following the high potentiality of lithium-bearing minerals generated from the processing and interpretation of LANDSAT 8 (OLI) images (Muavhi et al., 2023). Figure 4 shows the LANDSAT 8 (OLI) processing results for the project area.

The exploration technique employed includes:

1) Reconnaissance survey
2) Remote sensing
3) Field mapping
4) Geophysical survey, and
5) Preliminary geochemical sampling and analysis.

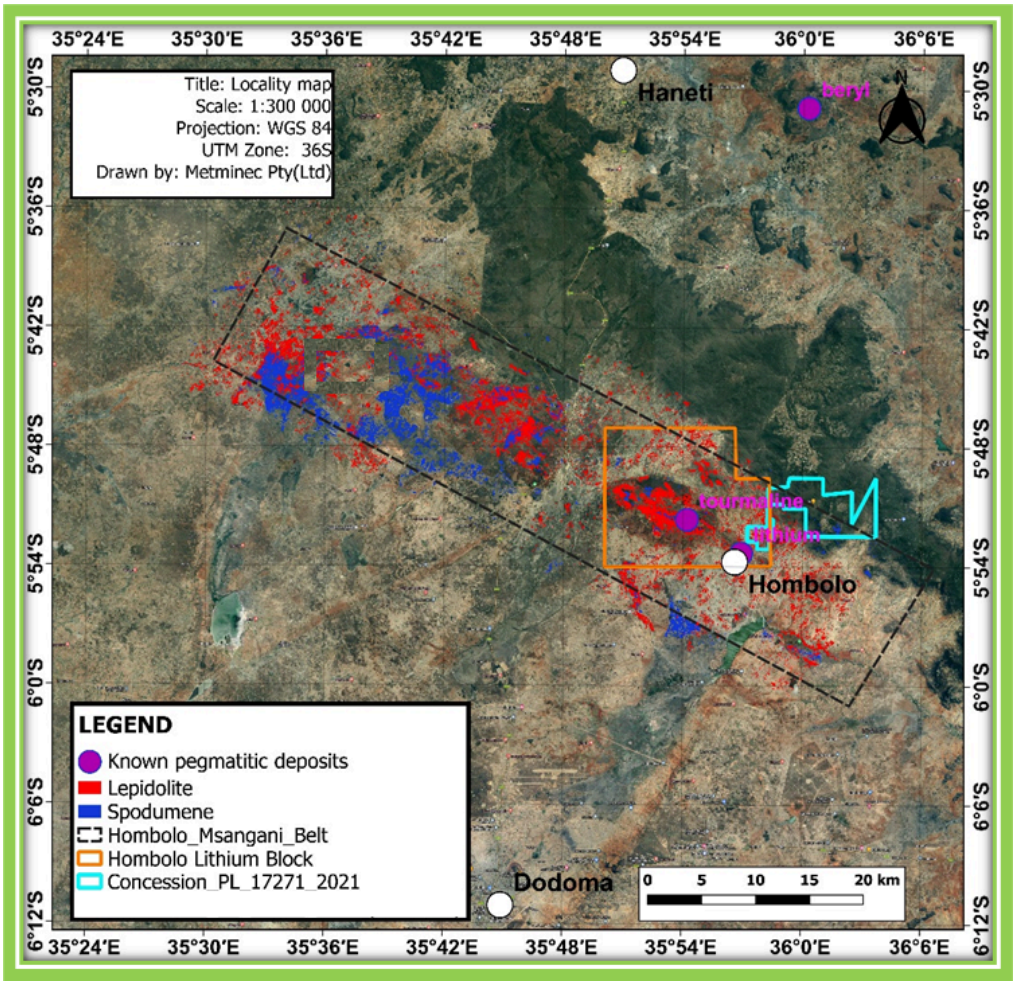

Figure 4: Potential lithium-bearing areas in the project area generated from the processing of LANDSAT images.

5.1. Reconnaissance survey

The desktop study and reconnaissance survey have been executed as part of the initial stages of the exploration program. The reconnaissance survey, as explained below, was aimed at familiarizing the exploration team with the concession area.

During the reconnaissance survey, it was discovered that the mountainous terrain, especially in the eastern part of the concession, is not favorable for both field mapping and geophysical survey. A site towards the southwest corner of the area which is flat-lying and easily accessible for field mapping and geophysical survey has been prioritized for immediate exploration work. This site also forms part of the Hombolo Lithium Block, a host to pegmatitic lithium deposits. In addition, the site is close to an active lithium mine to the west (See Figure 5). This block is approximately 500 ha.

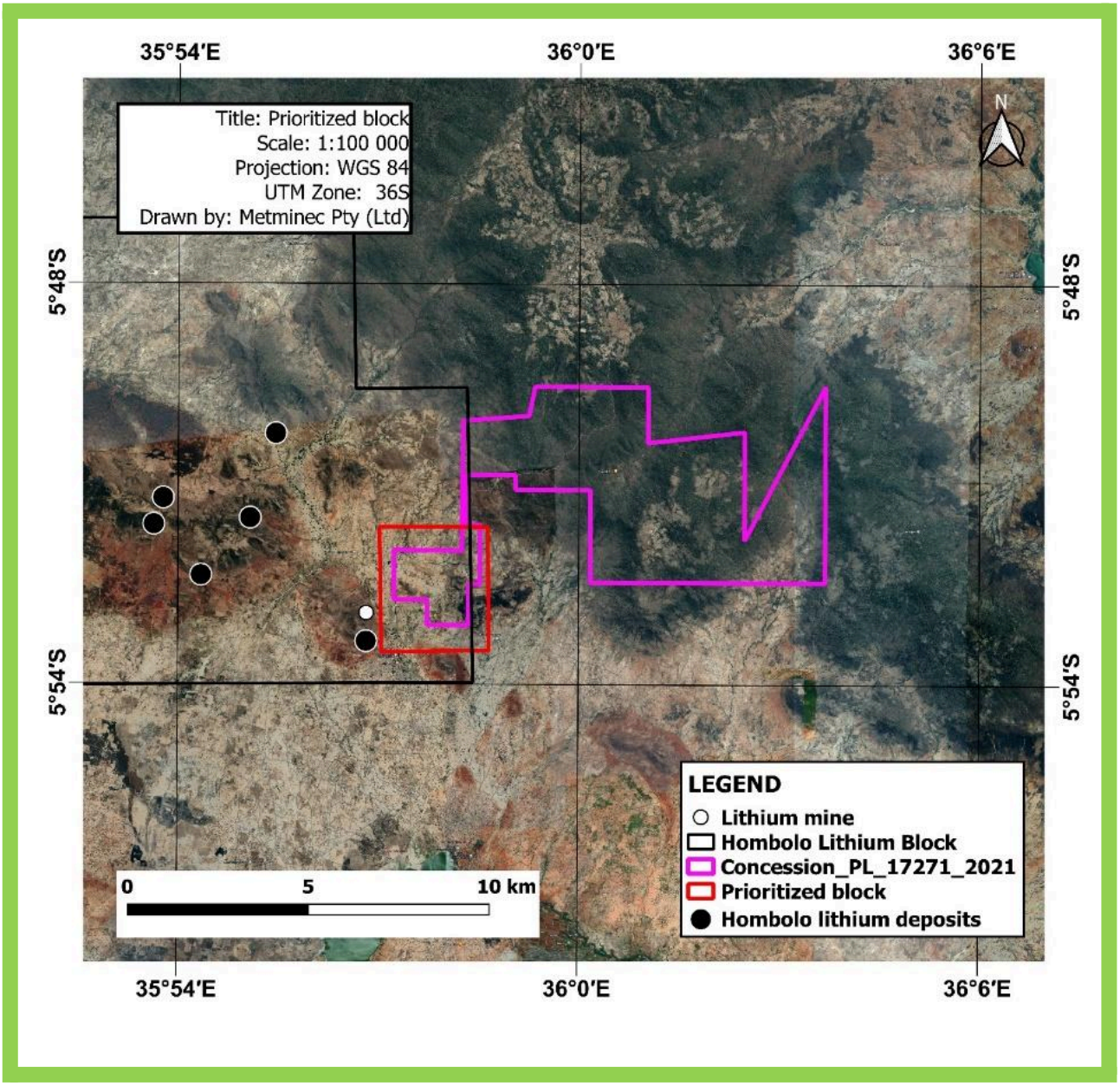

Figure 5: Prioritized block in red.

5.2. Field mapping and sampling

The main aim of field mapping was to locate and identify pegmatites and other lithological units that make up the geology of the prioritized block.

The block is characterized by outcrops of pegmatites, pegmatitic granites, porphyritic granite, and migmatites.

Figure 6 shows the predetermined traverse lines along which field mapping was conducted.

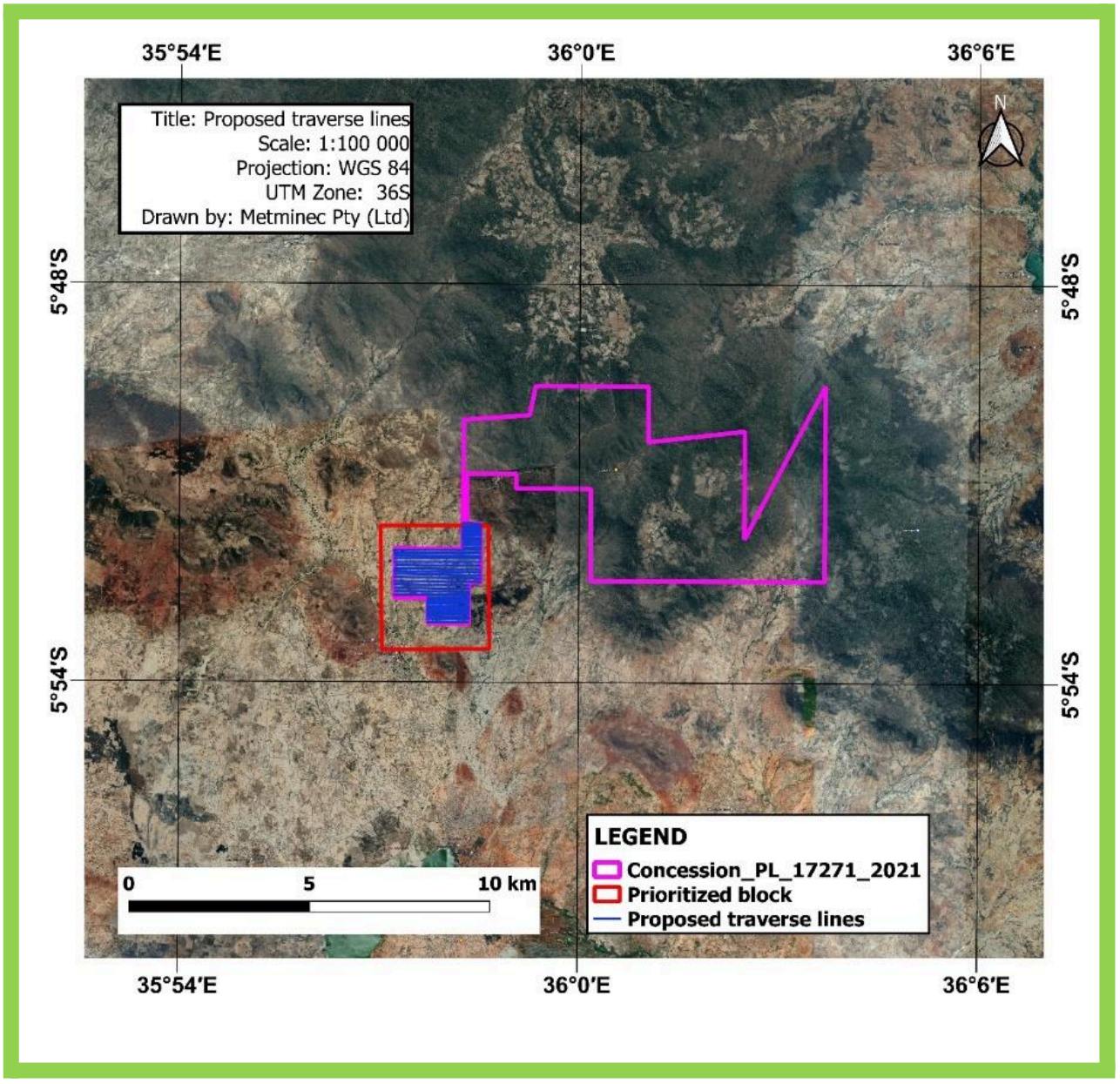

Figure 6: Predetermined traverse lines for field mapping.

Figure 7 shows some of the outcrops encountered during field mapping.

The full description of these outcrops, including the geological map generated following the findings of geological mapping, is given under the results section.

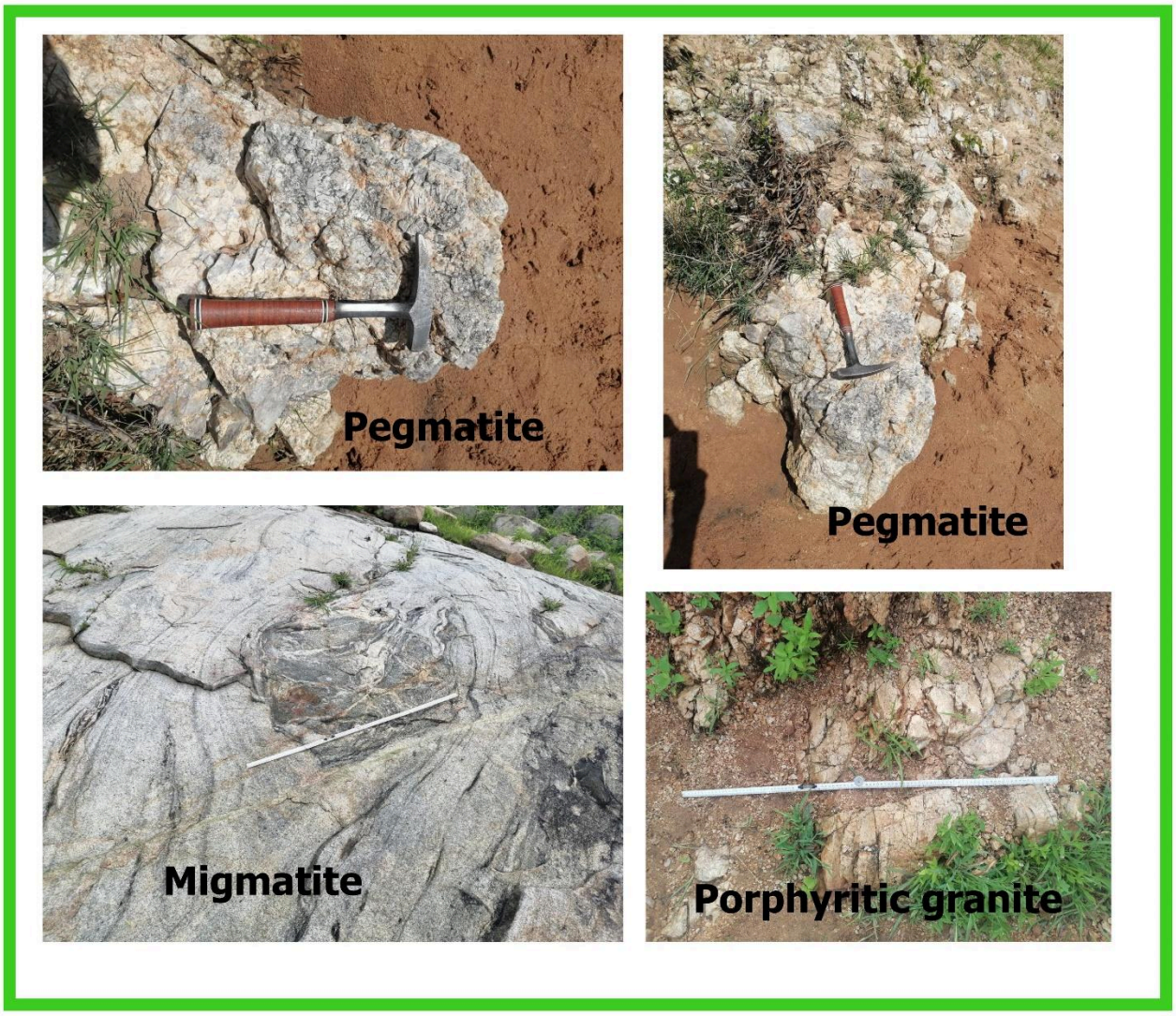

Figure 7: Some of the sampled outcrops (the lithologies entitled pegmatites are suspected pegmatites).

During field mapping, thirty-two rock samples were collected in the area (Figure 8).

These samples were collected in batches:

- The first batch comprising of twenty-four samples was collected in December 2023.
- The second batch consisting of eight samples was collected in January 2024.

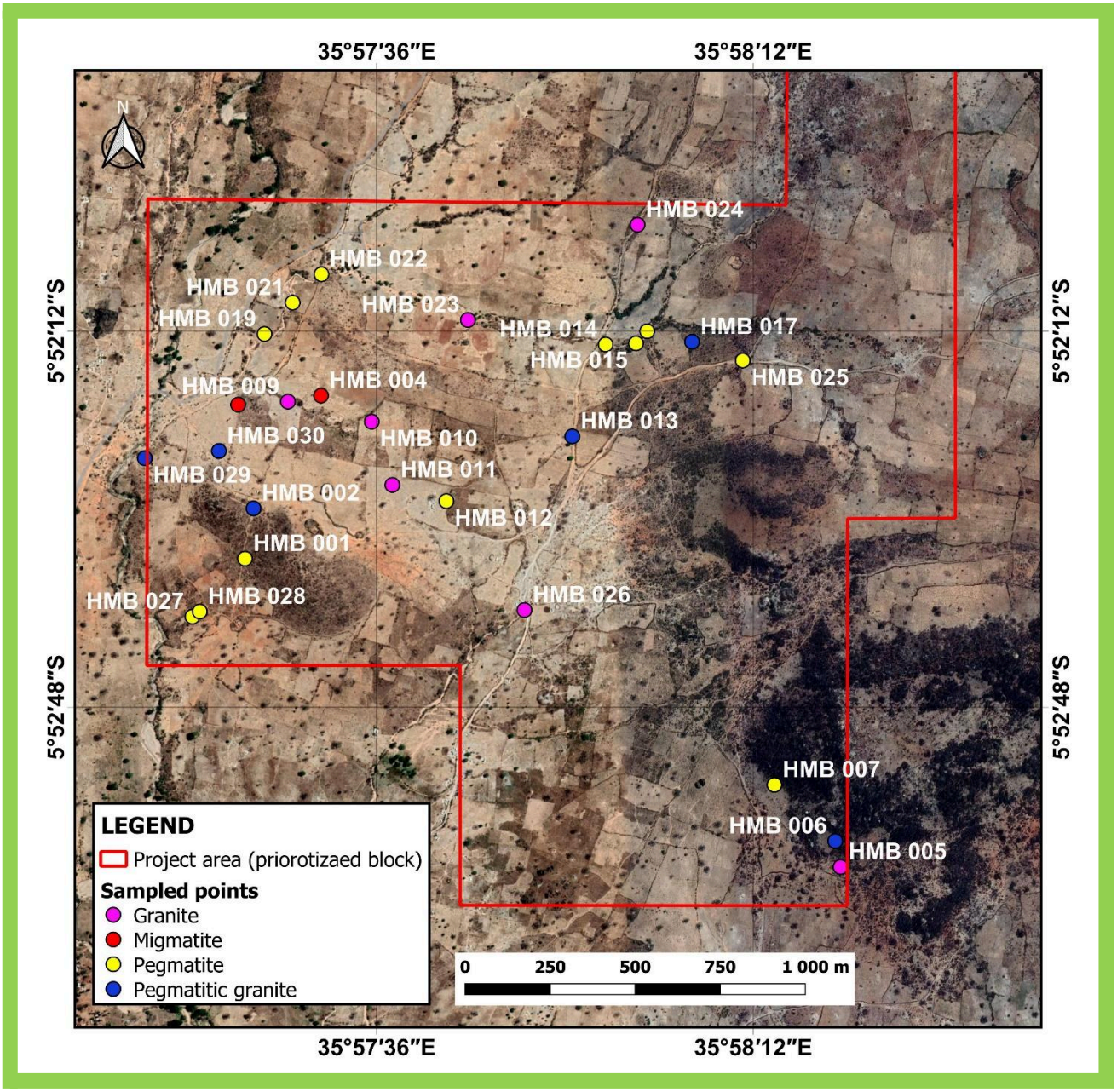

Figure 8: Sampled points to date.

5.3. Sample analysis

The purpose of conducting geochemical analysis is to determine whether the sampled rock types contain economically significant elements particularly Li and its main associated elements such as Ta, Cs, Nb, Be, etc.

At first, the following methods for analyzing lithium and associated metals were considered:

- ICPMS (Induced Coupled Mass Spectrometry) – for determining lithium content and whole rock geochemistry (major and trace elements).
- XRD (X-ray Diffraction) – for identifying different minerals

After conducting thorough research on reputable laboratories, it was evident that SGS Laboratory is renowned for its expertise and precision in analytical testing.

The laboratory in Mwanza (Tanzania) is affiliated with a reputable SGS Laboratory Group with laboratories based in South Africa, Australia, and Canada. However, the Mwanza SGS Laboratory has limitations as they do not have a setup to conduct full whole-rock geochemical analysis or mineralogical analysis, but they can perform the Inductively Coupled Plasma-Optical Emission Spectroscopy (ICP-OES) analysis method which can also be used for analyzing Li and some of the major and trace elements. The ICP-OES has been used in exploration all over the world (e.g., Vuollo and Honkamo, 2009; Drvodelic and Gagnon, 2023).

Twenty-four samples from the first batch were submitted to the Mwanza SGS Laboratory in December 2023 for major and trace element analysis using the ICP-OES technique.

Thereafter, the eight samples from the second batch were submitted to the laboratory in February 2024.

The analytical results of the first batch have been returned to the Metminec team, while those of the second batch are still pending. Consequently, the discussion of sample geochemistry in the results section below is limited to the samples from the first batch.

6. RESULTS

6.1. Field mapping results

A large part of the concession shown in the geological map (Figure 9) is covered by undifferentiated soil materials varying in color from reddish brown to grey. The concession is

characterized by pegmatites, granites, migmatites, granite porphyries, granitic gneisses, and isolated amphibolite in the shear zones. The heterogeneity in the grain size and mineral distribution and typical textures of pegmatitic granite such as intergrowths between quartz and K-feldspar are indicators of transition from granite, porphyritic granites, pegmatitic granite, and pegmatite.

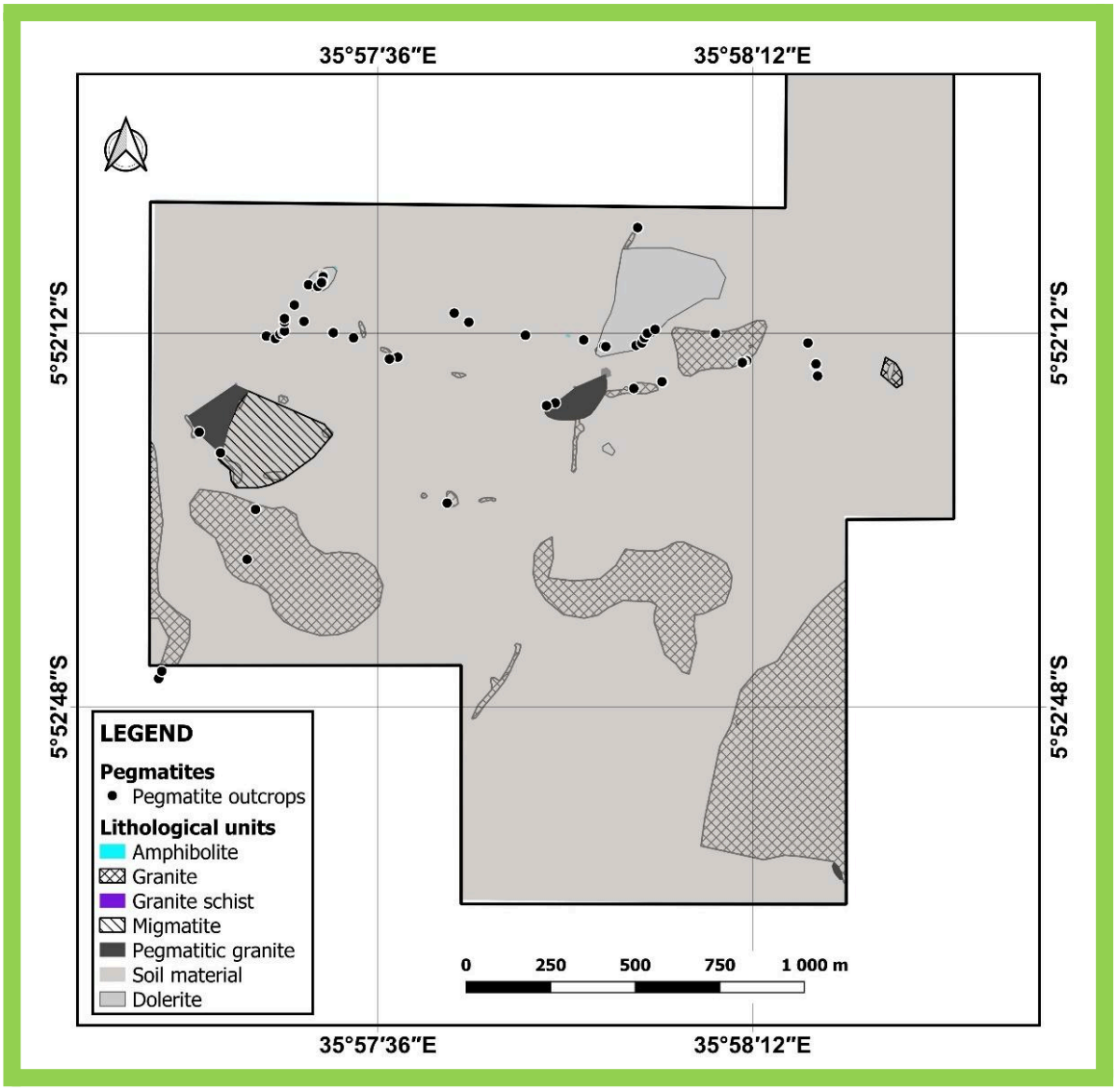

Figure 9: Geological map.

The project area is covered by undifferentiated soil. The soil is iron-rich and slightly magnetic in places. A significant change in geology is observed towards the north. This change is a result of many occurrences of dolerite intrusion that seems to be associated with the pegmatites which form a linear structure.

Different types of pegmatites occur in the area, granitic pegmatites, and feldspar-rich pegmatites. The area towards the southeastern corner of the concession is dominated by granite which forms part of the mountain and has the thick thorn bush. The southern part of the concession side of the con has little to no outcrop (Figure 10).

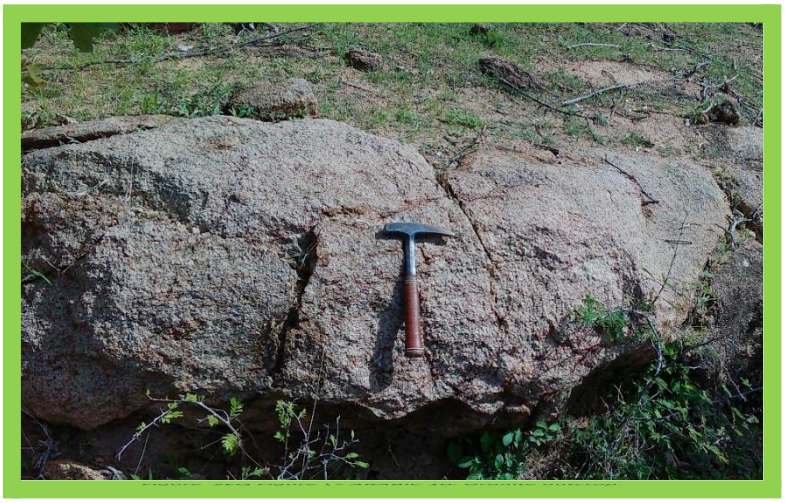

The porphyritic leucogranite found in the concession is predominantly characterized by k-feldspar crystals with minor Ca-feldspar. The feldspar crystal resembles a euhedral to the anhedral slope. The main mineral phases observed are Quartz, K-feldspar, and biotite. The crystals of quartz and K-feldspar size range between 2 cm to 4 cm. It has fine to medium-grained micas which are suspected to either be muscovite or biotite (Figure 11).

Figure 11: Porphyritic leucogranite outcrop.

The observed pegmatitic granite in the concession occurs in conjunction with porphyritic facies and pegmatite. The crystal's size is bigger and the rock becomes more or less equigranular as it transitions from porphyritic facies to pegmatitic granite. The mineral phases observed are quartz, K-feldspar, and biotite (Figure 12).

Figure 12: Pegmatitic granite.

The observed pegmatite (Figure 13 on the next page) found in the concession is associated with the silicified granite.

The pegmatites displayed a variety in terms of color and crystal size. In some places, they were a light color and pinkish in other areas.

The pegmatite is mainly observed in shear zones which are in contact with the dolerite and silicified granite. The pegmatites that are exposed in the stream appear to be strongly fractured and weathered and in places are associated with the amphibolite.

The thickness size of the pegmatite ranges from at least 4m to 20m. The observed main mineral phases of the pegmatite are quartz, K-feldspar, and mica.

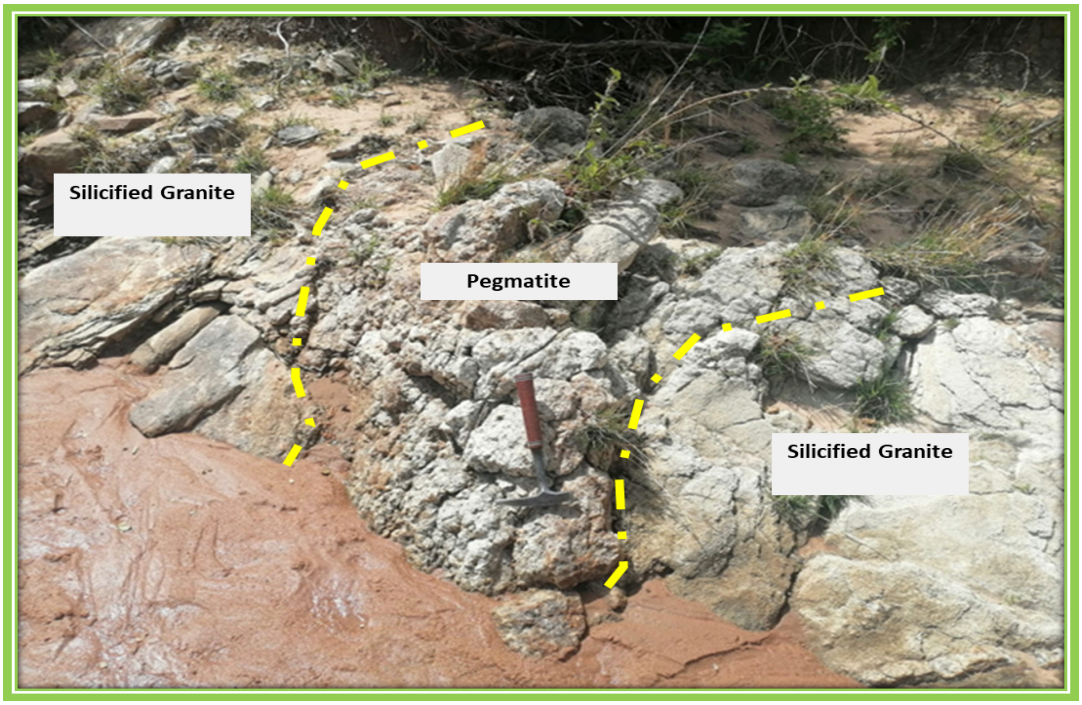

Figure 13: Pegmatite in contact with a silicified granite.

6.2. Geochemical results

Twenty-four samples from the first batch were analyzed for thirty-two major and trace elements (Al, As, Ba, Be, Ca, Cd, Co, Cr, Cu, Fe, K, La, Li, Mg, Mn, Mo, Ni, P, Pb, S, Sb, Sc, Si, Sn, Sr, Ti, V, W, Y and Zn) using the ICP-EOS analytic technique.

6.2.1. Assessment of potential lithium enrichment in the project area

Several elemental ratios have been utilized to assess the degree of fractionation which is responsible for the enrichment of rare element contents such as Li, Be, B, F, P, Ga, Rb, Cs, Y, Nb, Sn, REE, Ta, etc. In a fertile granitic system, ratios that are considered excellent fractionation indicators are K/Rb, K/Cs, Nb/Ta, Mg/Li, and K/Ba. Rare element pegmatites are characterized by significantly lower ratio values of K/Rb, K/Cs, Nb/Ta, and Mg/Li and a higher ratio of K/Ba than that of average upper continental crust or barren granitic systems (Černý and Meintzer, 1988; Selway and Breaks, 2005; Chukwu and Obiora, 2021; Chen et al., 2024). Considering the elements analyzed, only Mg/Li and K/Ba can be calculated from the ICP-OES results.

Out of twenty-four samples, twenty-two samples showed traces of Li contents with one sample (HMB 012) attaining the highest Li content of 44 ppm. The two samples that had Li content below the detection limit (10 ppm) of the used ICP-OES are HMB 005 and HMB 006.

Figure 14 below shows twenty-two samples with Li contents above the detection limit. Ten samples (HMB 003, HMB 011, HMB 012, HMB 019, HMB 021, HMB 022, HMB 023, HMB 024, HMB 025, and HMB 026) have Li contents of above 20 ppm; while the remaining twelve samples have Li contents in the range of 10 to 18 ppm.

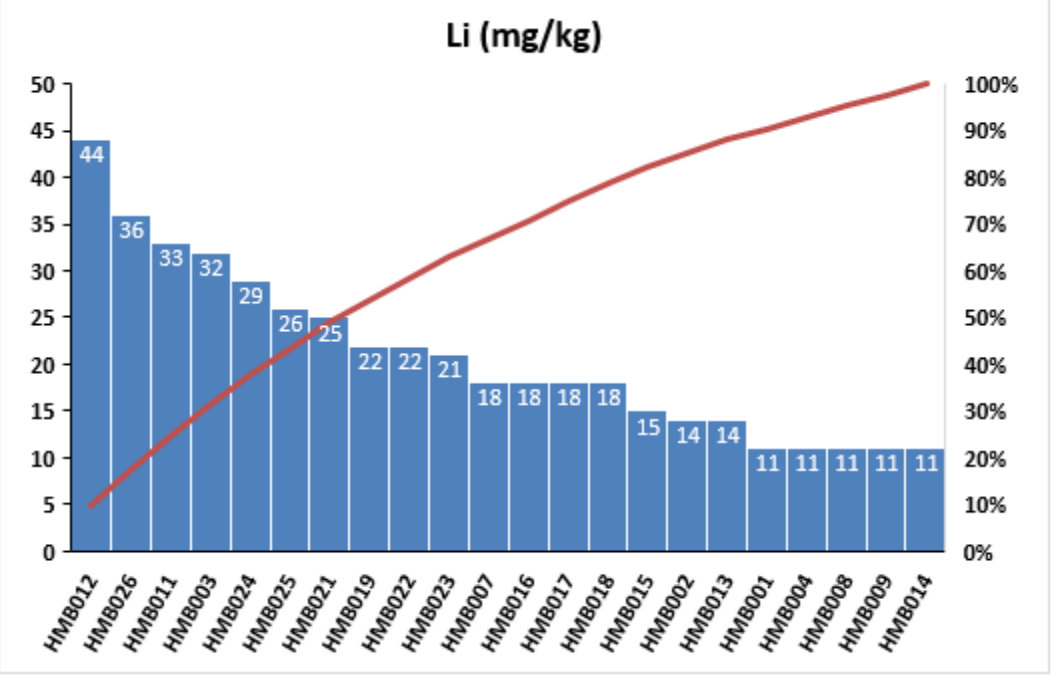

Figure 14: A bar graph showing the Li contents of the samples from the project area.

Following the previous work of Černý and Meintzer (1988), Selway and Breaks (2005), Chukwu and Obiora (2021), and Chen et al. (2024), the ratios that are considered excellent indicators of the fertile granitic system and rare element pegmatites were calculated for the samples of the current work (Table 3).

ID	Ba	Ca	K	Li	Mg	Mg/Li	K/Ba
HMB003	442	17000	16000	32	4300	134,4	36,2
HMB011	879	15000	27000	33	2000	60,6	30,7
HMB012	127	22000	11000	44	7600	172,7	86,6
HMB019	1869	700	45000	22	200	9,1	24,1
HMB021	1322	500	50000	25	500	20,0	37,8
HMB022	388	400	60000	22	300	13,6	154,6
HMB023	1590	800	41000	21	500	23,8	25,8
HMB024	432	300	35000	29	300	10,3	81,0
HMB025	727	300	42000	26	400	15,4	57,8
HMB026	950	12000	26000	36	1800	50,0	27,4
Li content below 20 ppm							
HMB001	1090	10000	3300	11	200	18,2	3,0
HMB002	740	12000	24000	14	900	64,3	32,4
HMB004	823	44000	32000	11	100	9,1	38,9
HMB005	1059	12000	27000	-	700	-	25,5
HMB006	2720	200	64000	-	100	-	23,5
HMB007	113	66000	800	18	61000	3388,9	7,1
HMB008	1099	10000	26000	11	700	63,6	23,7
HMB009	506	11000	14000	11	400	36,4	27,7
HMB013	1108	600	45000	14	100	7,1	40,6
HMB014	649	700	38000	11	400	36,4	58,6
HMB015	648	24000	29000	15	200	13,3	44,8
HMB016	915	400	49000	18	300	16,7	53,6
HMB017	591	800	42000	18	300	16,7	71,1
HMB018	228	900	22000	18	100	5,6	96,5
Rare element ratios in fertile granites and rare element pegmatites (Černý, 1989).						**1.7 – 50**	**48 – 18200**

Table 3: Selected elemental contents and ratio values of samples of the current work.

For better visualization of ratio values and identification of any existing elemental patterns, radar graphs were created (Figures 15 and 16).

From ten samples with > 20 ppm of Li contents, seven samples (HMB 019, HMB 021, HMB 022, HMB 023, HMB 024, HMB 025, and HMB 026) achieved Mg/Li ratio values in the range of 1 and 50 which is considered a good indication of increase in fractionation responsible for rare element enrichment in granitic rocks. Six of these samples (HMB 019, HMB 021, HMB 022, HMB 023, HMB 024, and HMB 025) are characterized by Mg/Li ratio values of < 25. The lower the Mg/Li ratio value the higher the potential of rare element enrichment in granites and pegmatites (Černý, 1989; Selway and Breaks, 2005; Chen et al., 2024). Sample HMB 026 attained the maximum acceptable Mg/Li value of 50. The Mg/Li ratio of >50 indicates abundant Mg which is mostly associated with barren granite (Selway and Breaks, 2005). Interestingly, this sample was collected in the southern half of the project area while the six samples with Mg/Li ratio values of < 25 were collected from streams to the north.

Samples: HMB 019, HMB 021, and HMB 022 were collected along the same stream segment covering a length of about 250 m from a sampling point of HMB 019 to the sampling point of HMB 022. These two samples attained relatively low Mg/Li ratios compared to the HMB 021 in the center of the stream segment. Their low-high-low Mg/Li ratio trend along the stream segment is well depicted in the radar graph (Figure 15).

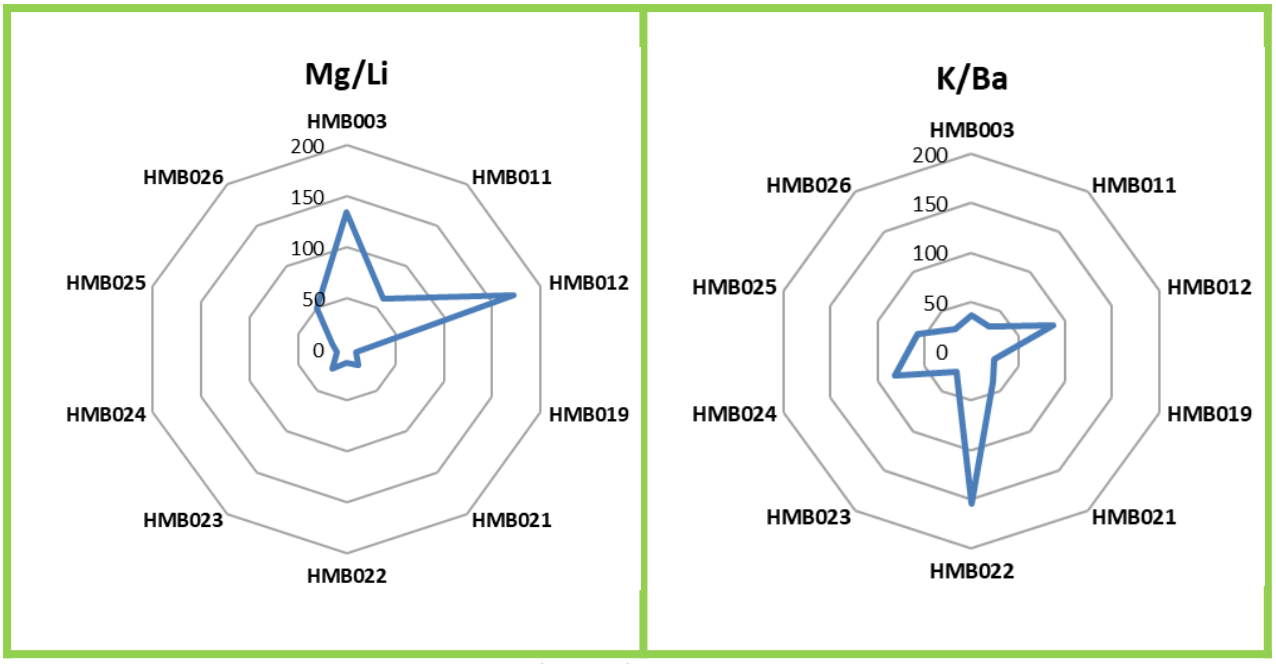

Figure 15: Radar graphs showing Mg/Li and K/Ba ratio values for samples with Li content of >20.

In addition, HMB 022 attained the highest K/Ba ratio value (174), another indicator of possible rare element enrichment. Fertile granite and rare element pegmatites are characterized by high values (> 48) whereas barren rock types are associated with low K/Ba values (Selway and Breaks, 2005). Other samples that attained both Mg/Li and K/Ba ratio values indicating potential enrichment are HMB 024 and HMB 025.

Despite being the sample with the highest Li content (44 ppm), HMB 012 achieved a Mg/Li ratio of 172 which is beyond the Mg/Li ratio range that indicates the increase of fractionation responsible for rare element enrichment in granitic rocks. High Mg content is associated with biotite gneiss, amphibolite, granites, gneiss, etc. (Chukwu and Obiora, 2021; Chen et al., 2024). Interestingly, this sample attained a K/Ba ratio of 86 which indicates low Ba content, a typical feature of fertile granite and rare element pegmatites (Selway and Breaks, 2005). HMB 012 attained the lowest Ba content out of all twenty-four samples from the first sample batch.

The pegmatite outcrop from which HMB 012 was collected is situated in the central part of the project area.

With respect to samples with Li contents of < 20 ppm, two (HMB 005 and HMB 006) out of fourteen samples have Li contents below the detection limit (10 pp) and as a result, the Mg/Li ratio values of the two samples could not be calculated.

From the twelve samples with Li contents above the detection limit, nine samples (HMB 001, HMB 004, HMB 009, HMB 013, HMB 014, HMB 015, HMB 016, HMB 017, and HMB 018) attained Mg/Li ratio values of < 50. Among the eight samples, seven samples (HMB 001, HMB 004, HMB 013, HMB 015, HMB 016, HMB 017, and HMB 018) have Mg/Li ratio values of < 20 and from these seven, three samples (HMB 004, HMB 013 and HMB 018) have very low Mg/Li ratio values of <10.

HMB 018 has the lowest Mg/Li ratio of 5.6 out of all twenty-four samples and as demonstrated by Selway and Breaks (2005) and others, a very low Mg/Li ratio indicates the potential of elevated Li contents in an evolved rock (fertile granite). In addition to this, HMB 018 attained the highest K/B ratio value (95) among the samples with Li contents below 20 ppm.

Other samples that attained both Mg/Li and K/Ba ratio values among the samples with Li contents of < 20 ppm include HMB 014, HMB 016, and HMB 017.

Samples (HMB 14, HMB 015, and HMB 016) were collected along the same stream segment. Meanwhile, the outcrop of HMB 017 lies about 100 m east of the stream segment. HMB 015, which is situated in the center of the stream segment length, attained the lowest Mg/Li ratio value among the three samples; thus, forming a high-low-high Mg/Li ratio trend (Figure 16) showing the trend observed along the three samples (HMB 019, HMB 021 and HMB 022) (Figure 15) with Li content of > 20 ppm.

Additionally, samples (HMB 14, HMB 015, and HMB 016) depict similar high-low-high K/Ba ratio trends as can be observed in the radar graph of K/Ba ratio values (Figure 16 on next page).

Sample HMB 14, HMB 015, and HMB 016 attained K/Ba ratio values of 58, 45, and 53,

respectively. This correspondence suggests that the outcrops along these stream segments may be of similar genetic origin.

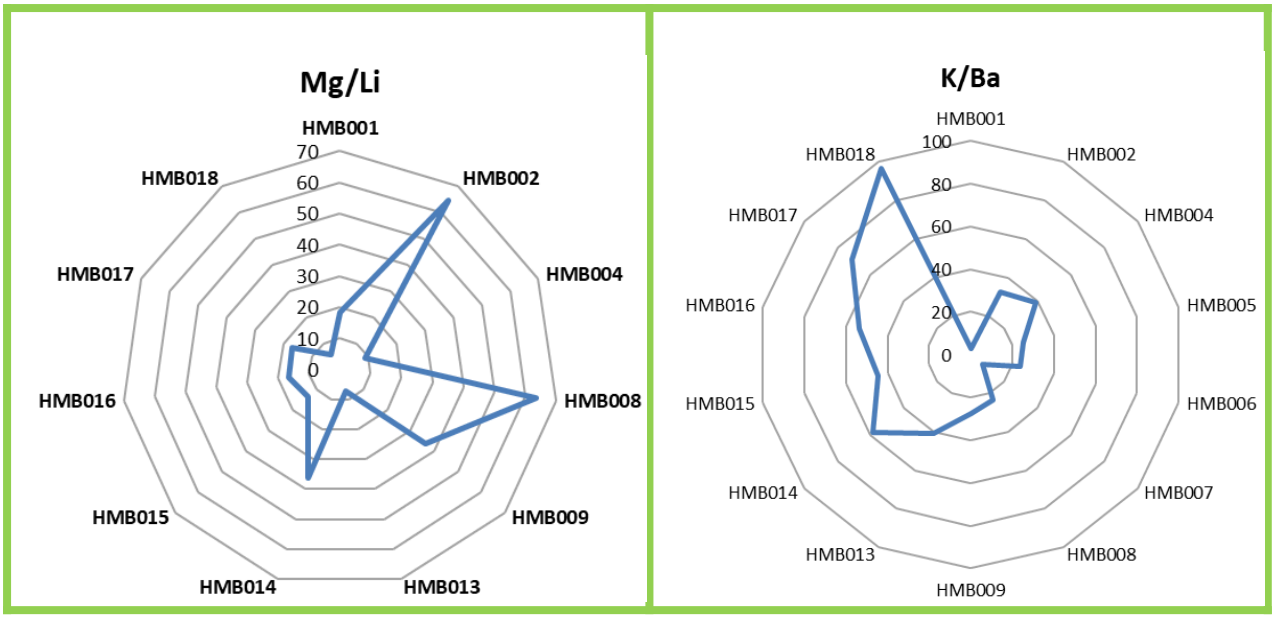

Figure 16: Radar graphs showing Mg/Li and K/Ba ratio values for samples with Li content of <20.

Out of twenty-four samples, HMB 007 has the highest Mg/Li ratio (3388,9) and the lowest K/Ba ratio of 7,1. In addition, the sample has the highest contents of major elements: Fe (8.1%), Ca (6.6%), Mg (6.1%), Ti (0.3%), and the lowest contents of major elements: Al (4.1%), K (0.8%) and Si (26.5%).

Major elements have been widely used to identify different rock types based on variability in major elemental geochemistry.

In general, rare element pegmatites and associated muscovite-rich granites have high K contents, and mafic or ultramafic rocks have high Ca contents while aplites have high Na contents (Selway and Breaks, 2005). Additionally, rare element pegmatites are characterized by relatively low Mg contents compared to barren pegmatites. As a result, various binary plots of major elements have been used to distinguish pegmatites from country rocks, including rare element pegmatites from barren pegmatite or granitic rocks.

The binary plots of K vs Ca and Mg vs Ca are displayed in Figures 17 and 18 that follow.

In addition, the geochemistry of pegmatites, granite gneiss, biotite gneiss, and amphibolite from

the study of Chukwu and Obiora (2021), and rare element pegmatites from Chen et al. (2024) were included in the plots for comparative purposes.

These studies were respectively conducted in southern Akwanga, North-Central Basement Complex of Nigeria, and Lijiagou Pegmatite Spodumene deposit in Western Sichuan, China. Note that the rare element pegmatites from these studies also show Mg/Li ratios below 50, meanwhile, biotite gneiss, amphibolite, and some granite gneiss show extremely high Mg/Li ratios which are associated with barren rocks (Černý and Meintzer, 1988) (See Table 4 on next page).

In the K vs Ca binary plot of samples with Li content of > 20 ppm, samples: HMB 003 and HMB 012 plot close to the trend of biotite gneisses from Chukwu and Obiora (2021). These samples have Ca content of above 15000 mg/kg. However, unlike HMB 003 which attained both Mg/Li and K/Ba values outside the fertile granitic zone, HMB 012 attained K/Ba value within the potential fertile zone in addition to the highest Li content.

Sample HMB 024 plots at one of the rare element pegmatites from the previous study. Also, HMB 024 attained the Mg/Li and K/Ba ratio values indicating potential rare element enrichment. In general, all samples plot towards the K axis (except HMB 003 and HMB 012) where most pegmatites and granite gneisses from previous studies are concentrated.

The sample which is slightly off of this trend is HMB 011. Sample HMB 011 and HMB 003 are the only samples with both Mg/Li and K/Ba ratio values outside the potential rare element enrichment zone.

In the Mg vs Ca binary plot of samples with Li content of > 20 ppm, sample HMB 012 plots close to granite gneiss from Chukwu and Obiora (2021).

Interestingly, HMB 011, HMB 003, and HMB 012 show an increasing trend of Mg and Ca content (Figure 17).

Samples: HMB 011 and HMB 012 were collected close to each other and that may contribute to the observed similarities in elemental behavior.

The remaining samples correspond to pegmatites and granite gneiss of previous studies.

ID	Ba	Ca	K	Li	Mg	Mg/Li	K/Ba
CA01 (RE Pegmatite)	14	2216	29802	101	603	6,0	2128,7
CA02 (RE Pegmatite)	19	786	47319	27	1287	47,7	2490,5
CA03 (RE Pegmatite)	31	1215	35032	30	483	16,1	1130,1
CA04 (RE Pegmatite)	28	2501	26150	42	543	12,9	933,9
CA05 (Re Pegmatite)	21	3788	16935	29	724	25,0	806,4
CA06 (RE Pegmatite)	11	858	37108	66	2473	37,5	3373,5
CA07 (Pegmatite)	112	6218	27976	5	121	24,2	249,8
CA18 (Pegmatite)	10	4574	32293	31	362	11,7	3229,3
CA19 (Pegmatite)	571	12364	22082	40	1025	25,6	38,7
CA23 (Granite gneiss)	577	4360	45102	30	965	32,2	78,2
CA24 (Granite gneiss)	928	8719	46488	71	1508	21,2	50,1
CA25 (Granite gneiss)	1623	9648	44330	70	3257	46,5	27,3
CA28 (Granite gneiss)	891	21012	25154	89	5911	66,4	28,2
CA37 (Granite gneiss)	631	5932	49809	27	664	24,6	78,9
CA40 (Granite gneiss)	1303	9291	44164	19	2352	123,8	33,9
CA29 (Biotite gneiss)	1570	35378	29138	90	14236	158,2	18,6
CA38 (Biotite gneiss)	307	8362	1749	36	36610	1016,9	5,7
CA30 (Amphibolite)	151	83405	69187	80	9298	116,2	458,2
Ave. RE Pegmatite*	2	2287	21584	10265	543	0,1	10792,0
Ave. Pegmatite*	13	3502	32044	228	1821	8,0	2464,9

Table 4: Selected major and trace elements and ratios of different rock types from Chukwu and Obiora (2021) and Chen et al. (2024).

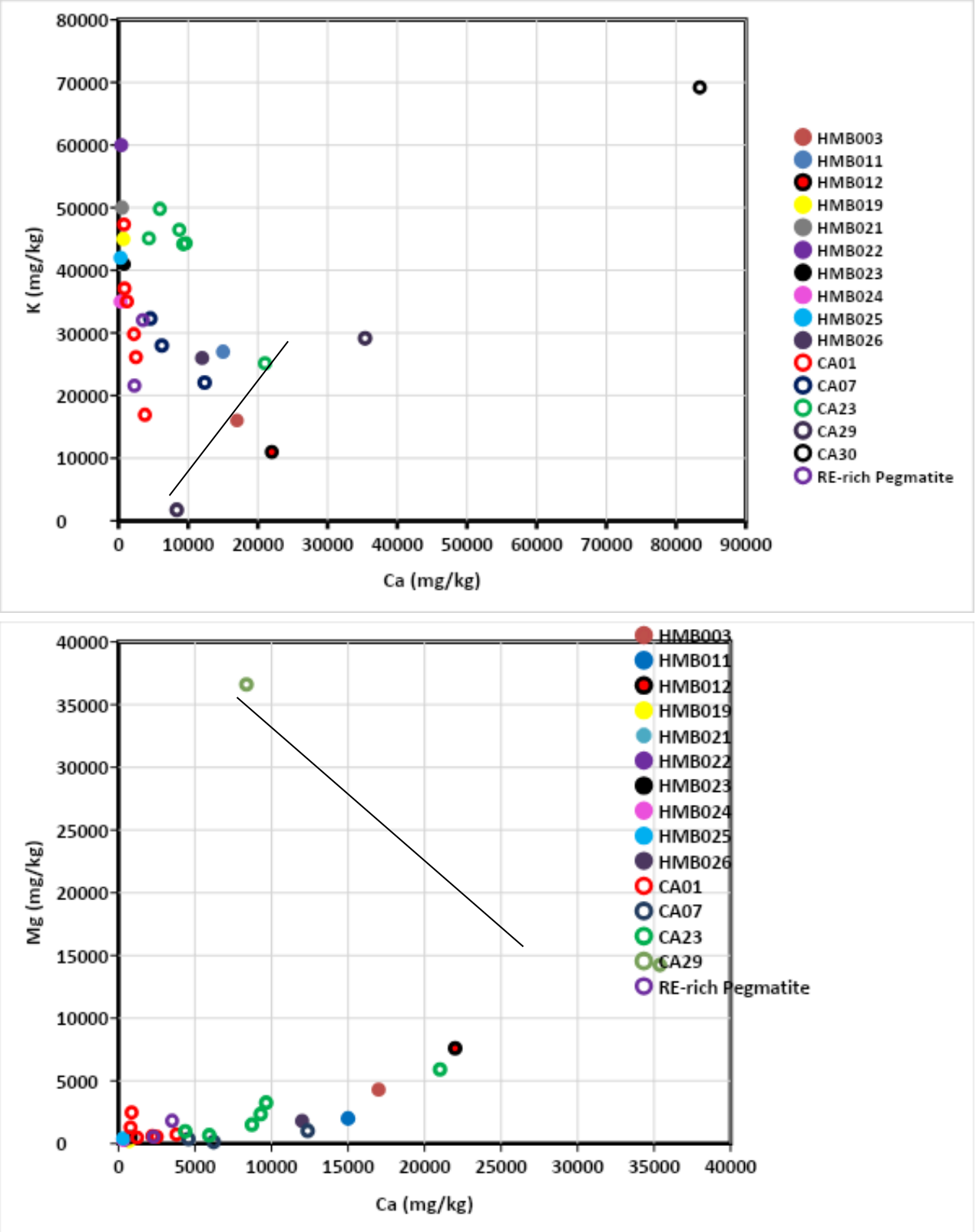

Figure 17: K vs Ca and Mg vs Ca binary plots of samples with Li content of > 20 ppm. The black line represents the biotite gness trend from Chukwe and Obiara (2021).

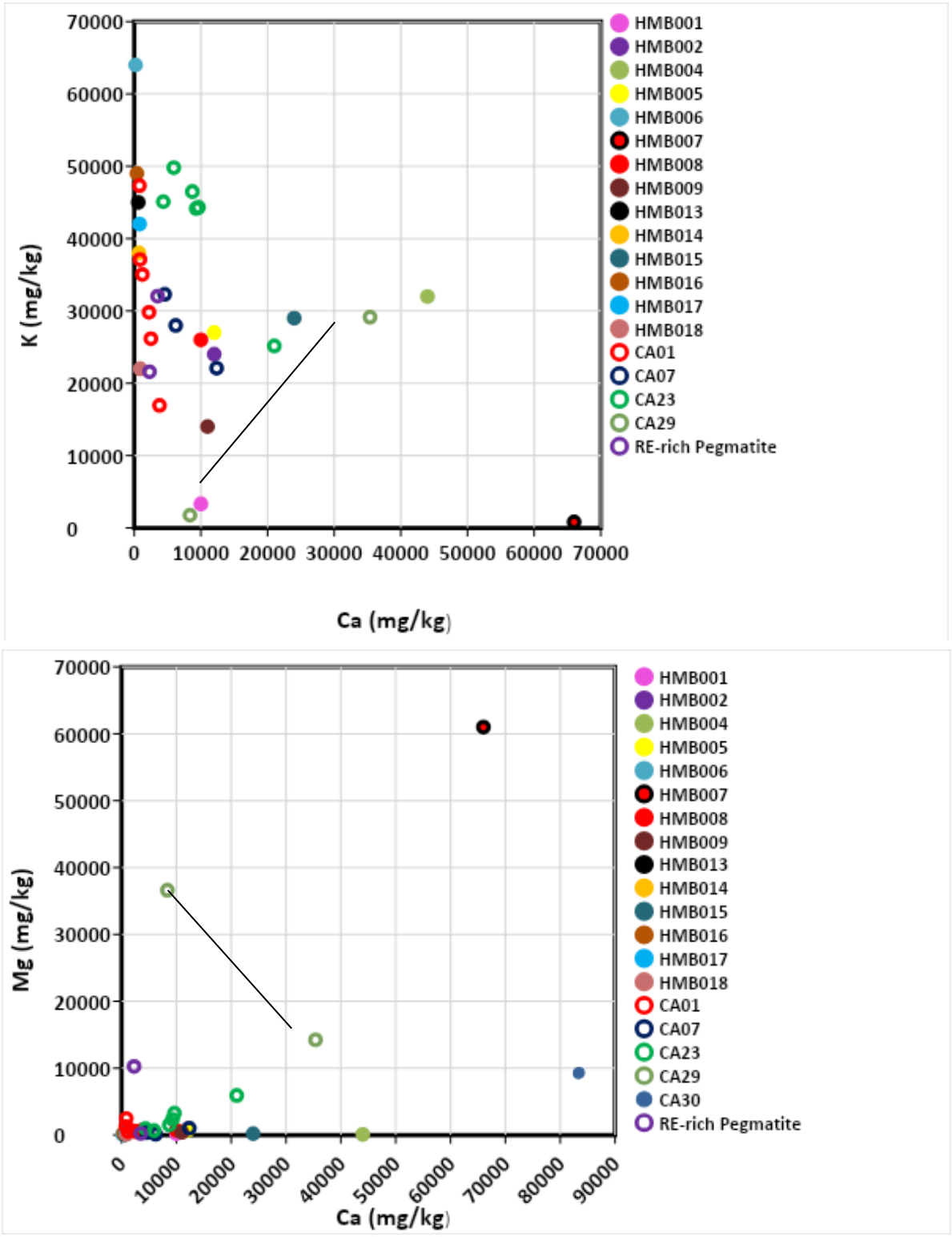

Figure 18: K vs Ca and Mg vs Ca binary plots of samples with Li content of < 20 ppm.

In the K vs Ca binary plot of samples with Li content of < 20 ppm, it is clear that HMB 007 is not related to the rock types in the plot. HMB 007 is the same sample that attained uniquely high major elemental contents.

Likewise, HMB 006 appears to be isolated from other samples including the rock types in the plot. HMB 006 is one of the two samples with Li content below the detection limit of 10 ppm. This sample was collected proximal to the sampling point of HMB 007, but the discrepancies in Ca and K contents between the two samples are astounding (Figure 18).

On the other hand, HMB 018 and HMB 014 correspond to the K and Ca contents of the rare element pegmatite of Chen et al. (2024) and Chukwe and Obiara (2021), respectively. The two samples attained Mg/Li and K/Ba values which indicate potential rare element enrichment. Another sample that fits this category (HMB 016) plots close to pegmatite from Chukwe and Obiara (2021).

In the Mg vs Ca plot, most samples correspond to pegmatite and granites of the previous study. Sample HMB 007 is still isolated depicting its extremely elevated major elemental geochemistry (Figure 18).

6.2.2. Assessment of potential enrichment of other economic metals in the project area

During the assessment of geochemical results, it was noticed that some of the samples depict elevated contents of some of the critical and strategic metals.

For instance, seven samples (HMB004, HMB009, HMB015, HMB016, HMB017, HMB021, HMB024) show traces of Be (above the detection limit of 5 ppm) (See Table 5 on next page).

Elevated Be contents are associated with rare element enrichment in pegmatites (Černý and Meintzer, 1988; Selway and Breaks, 2005; Chukwu and Obiora, 2021; Chen et al., 2024).

Four Samples with traces of Be (HMB 015, HMB 016, HMB 017, HMB 021, and HMB 024) attained Mg/Li and K/Ba values indicating potential rare element enrichment.

ID	Be (ppm)
HMB004	10
HMB009	5
HMB015	10
HMB016	10
HMB017	5
HMB021	10
HMB024	10
The average crustal abundance of Be is 3 ppm (Taylor and McLennan, 1985).	

Table 5: Samples with traces of Be.

In addition, HMB 024 is one of the two samples (the other being HMB 007) out of all samples with Sn contents above the detection limit of 50 ppm. Sample HMB 024 has a Sn value of 59 ppm which is quite significant considering the average crustal abundance of Sn (5.5 ppm) (Taylor and McLennan, 1985).

Figure 19 shows a pie diagram of three critical/strategic metals from HMB 024. The sample recorded Li content of 29 ppm, Be of 10 ppm, and Sn of 59 ppm. Also, this sample in the K vs Ca binary plot corresponds to the K and Ca contents of one of the rare element pegmatites from Chukwe and Obiara (2021).

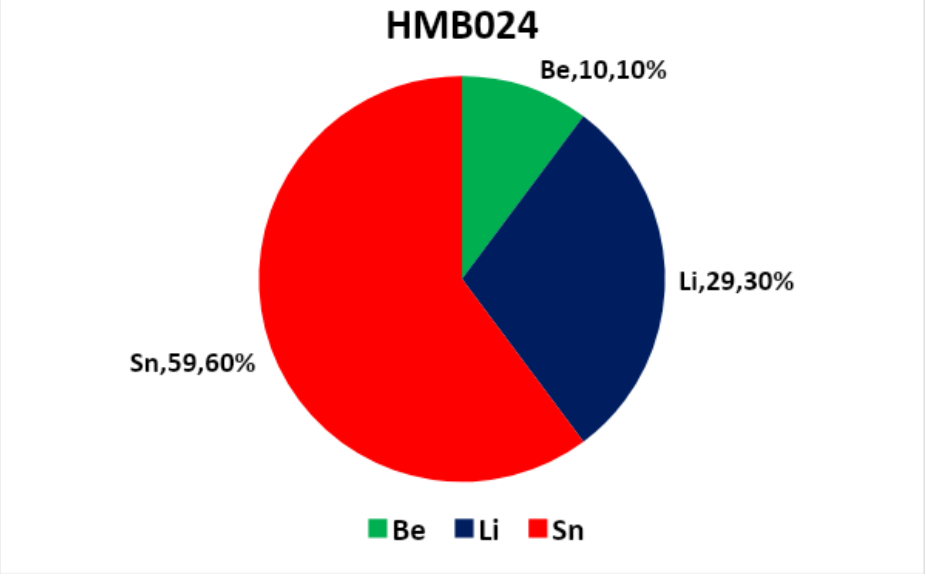

Figure 19: Pie diagram showing contents of critical/strategic metals from sample HMB 024.

Meanwhile, HMB 007 has the highest contents of Sn, Y, and Sc out of twenty-four analyzed samples. A pie diagram showing the contents and percentages of four critical metals (Li, Y, Sc, and Sn) from HMB 007 is shown in Figure 20.

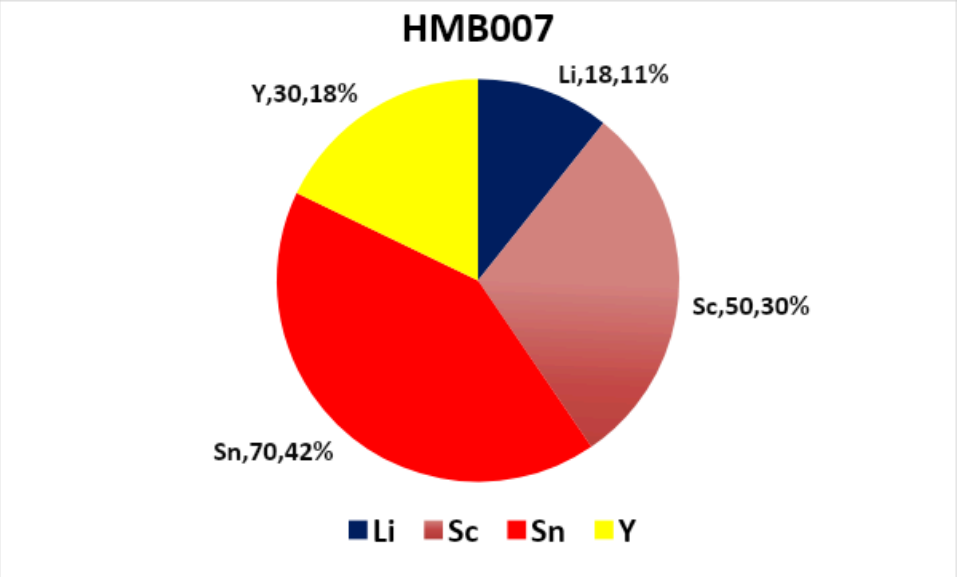

Figure 20: Pie diagram showing contents of critical metals from sample HMB 007.

According to Coetzee (1984), Sn value as high as 35 ppm is considered a good indicator of a potential Sn ore. Meanwhile, Olade (1980) indicated that regardless of the inherent erratic nature of Sn content, a Sn value exceeding 25 ppm provides criteria for recognizing Sn-bearing zones in granite. In this premise, the Sn contents of HMB 024 and HMB 007 present a potential to recognize existing Sn-bearing zones in their outcrops.

As stated previously, HMB 007 has the highest Y content out of twenty-four analyzed samples. Other samples with Y contents above the detection limit of 5 ppm include HMB 001, HMB 003, HMB 004, HMB 009, HMB 012, HMB 014, HMB 015, and HMB 018 (Figure 21 on next page).

According to (Černý, 1989), fertile granites and rare element pegmatites have Y contents in the range of 3 to 103 ppm. Yttrium is also one of the major elements of NYF pegmatite, the counterpart of LCT pegmatite (Duuring, 2020).

Among the samples with traces of Y, HMB 018 and HMB 014 have Mg/Li and K/Ba values attained Mg/Li and K/Ba values indicating potential rare element enrichment. These samples also

correspond to the K and Ca contents of the rare element pegmatite of Chen et al. (2024) and Chukwe and Obiara (2021), respectively.

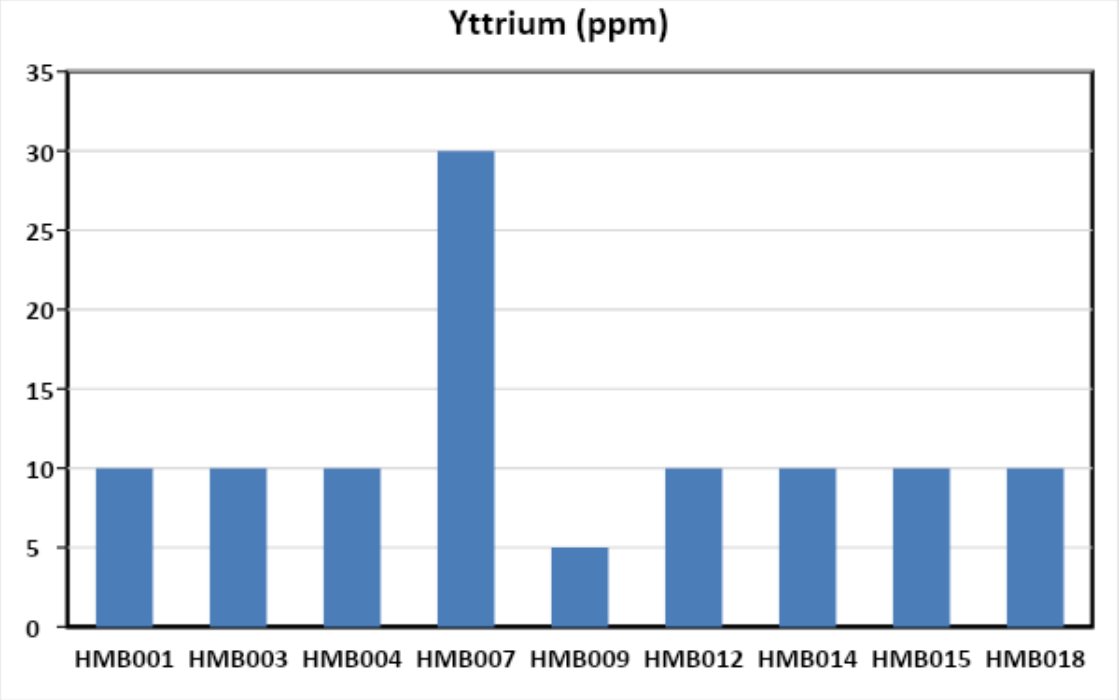

Figure 21: Bar graph of Yttrium contents.

7. CONCLUSIONS

The analysis of whole-rock geochemistry of rock samples is considered an excellent tool to distinguish between barren granite and fertile granite and to evaluate the degree of fractionation which is responsible for rare element enrichment in pegmatites.

Ratios that are considered excellent fractionation indicators of rare element enrichment are K/Rb, K/Cs, Nb/Ta, K/Ba, and Mg/Li. Considering the elements analyzed, owing to the limitations inherent to ICP-OES used in Mwanza SGS Laboratory, only Mg/Li and K/Ba ratio values were calculated.

The limitations include the inability of the analytical technique to measure the contents of Rb, Cs, Nb, Ta and other Li associated elements and elements essential for proper petrological classification.

Out of twenty-four analyzed samples, twenty-two samples show traces of Li content with HMB 012 attaining the highest Li content (12 ppm). Most samples have Mg/Li and K/Ba ratios within the range that indicate potential rare element enrichment. These include HMB 014, HMB 016, HMB 017, HMB 018, HMB 022, HMB 024, HMB 025. Also, some of these samples correspond to Mg, K, and Ca contents of known rare element pegmatites (from previous studies) in Ca vs K and Mg vs Ca binary plots. In addition, HMB 024 and HMB 007 showed some high contents of Sn. Tin value as high as 35 ppm is considered a good indicator of a potential Sn ore. Therefore, the Sn contents of HMB 024 and HMB 007 may present a potential to recognize existing Sn-bearing zones in their outcrops.

Although the results do not permit a comprehensive understanding of the geological context of the collected samples, they do, however, provide preliminary insights towards the existing potential of rare element enrichment associated with the increase in degree of fractionation in the area.

8. RECOMMENDATIONS

It is recommended to conduct follow-up sampling and trenching (or drilling) at points displaying traces of Li and critical metals.

Considering the advantages of ICP-MS over ICP-OES below:

- ICP-MS can analyze a wider elemental range compared to ICP-OES.
- ICP-MS offers lower detection limits making it more sensitive for trace elemental analysis.
- This technique can detect elements at a part per trillion (ppt).
- ICP-MS has relatively high precision and accuracy compared to ICP-OES.

Metminec recommends that the samples be sent to South Africa to be analyzed at the SGS Laboratory utilizing the ICP-MS instrument. ICP-MS provides high precision and accuracy of element analysis. All targeted elements except for fluorine will be able to be measured.

In addition, given lithium reactivity and difficulty in detection from surface outcrops, it is also advisable to focus the analyses more on its associated elements for a comprehensive understanding of the geological context. This further justifies the use of ICP-MS which can detect

a wide range of elements as compared to ICP-OES.

We also recommend the use of the XRD (X-ray diffraction) analytical technique in addition to the ICP-MS technique. XRD is useful in identifying and quantifying minerals and rock samples. This should also be done at the SGS Laboratory in South Africa since the SGS Laboratory in Tanzania does not possess XRD.

It is further recommended that test holes be drilled at specific target points (sites) to define and better understand the geology of the area. The core samples will be logged in detail and samples will be sent to the laboratory in South Africa to conduct IPCMS and XRD analysis on the core samples.

9. REFERENCES

Ali, A. and Pour, A. (2014). Lithological mapping and hydrothermal alteration using Landsat 8 data: a case study in Ariab mining district, Red Sea Hills, Sudan. Int. J. Basic Appl. Sci. 3(3).

Andualema, T.C. and Demeke, G.G. (2019). Groundwater potential assessment using GIS and remote sensing: A case study of Guna tana landscape, upper Blue Nile Basin, Ethiopia. Journal of Hydrology: Regional Studies, 24, 1-13. https://doi.org/10.1016/j.ejrh.2019.100610

Arshad, A., Zhang, Z., Zhang, W., and Dilawar, A. (2020). Mapping favorable groundwater potential recharge zones using a GIS-based analytical hierarchical process and probability frequency ratio model: A case study from an agro-urban region of Pakistan. Geoscience Frontiers, 11(5), 1805-1819. https://doi.org/10.1016/j.gsf.2019.12.013

Breaks, F.W. and Tindle, A.G., 1997. Rare element exploration potential of the Separation Lake area: An emerging target for Bikita-type mineralization in the Superior province of northwest Ontario. In Summary of Field Work and Other Activities 1997. Ontario Geological Survey, Miscellaneous Paper 168, p. 72-88.

Černý, P., 1989a. Exploration strategy and methods for pegmatite deposits of tantalum. In Lanthanides, Tantalum, and Niobium. Edited by P. Moller, P. Černý and F. Saupe. Springer-Verlag, New York, p. 274-302.

Černý, P. and Meintzer, R.E., 1988. Fertile granites in the Archean and Proterozoic fields of rare element pegmatites: Crustal environment, geochemistry, and petrogenetic relationships. In Recent Advances in the Geology of Granite-related Mineral Deposits. Canadian Institute of Mining and Metallurgy, Special Publication 39, p. 170-206.

Chen, X.; Chen, C.; Lai, X.; Yang, Y.; Gu, Y.; Cai, Y. (2024). Whole-Rock Geochemistry and Mica Compositions in Lijiagou Pegmatite Spodumene Deposit, Western Sichuan, China. Minerals, 14, 69. https:// doi.org/10.3390/min14010069.

Chukwu, A. and Obiora, S.C. (2021). Petrogenetic characterization of pegmatites and their host rocks in southern Akwanga, North-Central Basement Complex, Nigeria. J. Earth Syst. Sci.., 130(18), p1-23.

CML (2022). Chenene Project. Accessed from http://www.cassiusmining.com/operations/tanzania/#:~:text=The%20Chenene%20Lithium%20Project%20consists%20of%20four%20contiguous,the%20annual%20wet%20season%20than%20areas%20further%20south.

Deberitz, J. (1993). Lithium. Verlag Moderne Industrie AG & Co., Landsberg/Lech., Germany, 70p.
Dill, H.G. Pegmatites and aplites: Their genetic and applied ore geology. Ore Geol. Rev. 2015, 69, p417–561.

Duuring, P. (2020). Rare-element pegmatites: A mineral systems analysis. Geological Survey of Western Australia, Record 2020/7, p6.

Fernandes, J.C., Teodoro, A.C. and Lima, A. (2019). Remote sensing data in lithium (Li) exploration: A new approach for the detection of Li-bearing pegmatites.

Gagnon, M-A and Drvodelic, Ni. (2023). Assay of Alkali Metals in Pegmatite and Spodumene Ores by ICP-OES.

Garrett, D.E. (2004). Handbook of Lithium and Natural Calcium Chloride, Lithium, 235p. doi:10.1016/B978-012276152-2/50037-2.

Green, A.A., and Craig, M.D. (1985). Analysis of aircraft spectrometer data, with logarithmic residuals: Proceedings of the Airborne Imaging Spectrometer Data Analysis Workshop, 111-119.

Karashani, B. (2023). US firm joins rush for new lithium deposits in Tanzania. https://www.theeastafrican.co.ke/tea/business/us-firm-joins-rush-for-tanzania-lithium-deposits-4157856.

Kokaly, R.F., Clark, R.N., Swayze, G.A., Livo, K.E., Hoefen, T.M., Pearson, N.C., Wise, R., Benzel,

W.M., Lowers, H.A., Driscoll, R.L., and Klein, A.J. (2017). USGS Spectral Library Version 7: U.S. Geological Survey, Data Series

Linnen, R.L., Van Lichtervelde, M. and Cerny, P. (2012). Granitic Pegmatites as Sources of Strategic Metals. Elements, 8(4), 275-280. doi:10.2113/gselements.8.4.275 .

London, D. Granitic pegmatites: An assessment of current concepts and directions for the future. Lithos 2005, 80, p281–303.

London, D. (2008). Pegmatites: The Canadian Mineralogist Special Publication, 10, p347.

Mat, M. (2023). Lithium (Li) Ore. Accessed from [https://geologyscience.com/ore-minerals/lithium-li-ore/#:~:text=The%20most%20common%20lithium-bearing%20minerals%20found%20in%20lithium,found%20in%20igneous%20rocks%2C%20pegmatites%2C%20and%20sedimentary%20deposits].

Muavhi. N, Mavhungu, M.E. and Ndivhudzannyi, R. (2021). Mapping of potential rare earth deposits in the Schiel Alkaline Complex using Sentinel 2 MSI. Egypt Journal of Remote Sensing and Space Science, 24(3), 609-617.

Muavhi, N., Shingage, P. and Mosala, T. C. (2023). The desktop study report on lithium deposit exploration in Tanzania, 37p.

Sabins, F.F. (1999). Remote sensing for mineral exploration. Ore Geology Reviews, 14, 157–183.

Selway, J.B and Breaks, F.W. (2005). A Review of Rare-Element (Li-Cs-Ta) Pegmatite Exploration Techniques for the Superior Province, Canada, and Large Worldwide Tantalum Deposits. Exploration and Mining Geology, Vol. 14, Nos. 1-4, pp. 1-30.

Steiner, B.M. (2019. Tools and Workflows for Grassroots Li–Cs–Ta (LCT) Pegmatite Exploration. Minerals, 9, 1-23. doi:10.3390/min9080499.

Von Knorring, O. and Condliffe, E. (1987). Mineralized pegmatites in Africa. Geological Journal, Thematic Issue, 22, 253-270.

Vuollo, P., Honkamo, J., Niemelä, M., Perämäki, P. and Jantunen, H. (2009). Determination of boron and lithium in ferroelectric samples by ICP-OES and ICP-MS. Microchimica Acta, 164, 217-224.